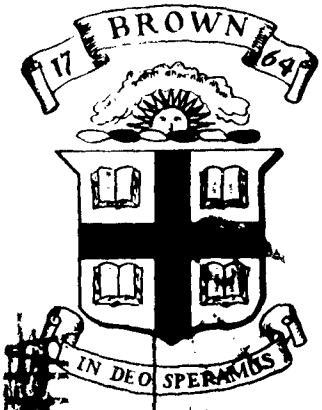

Division of Engineering
BROWN UNIVERSITY
PROVIDENCE, R. I.

THE BEHAVIOR OF METALS AT ELEVATED TEMPERATURES UNDER IMPACT WITH A BOUNCING BALL

BY

C. H. MOK and J. DUFFY

Department of the Navy
Office of Naval Research
Contract Nonr 562(20) NR-064-424
Technical Report No. 33

Nonr-562(20)/33

April 1963

The Behavior of Metals at Elevated Temperatures under Impact with a Bouncing Ball

by

C-H. Mok and J. Duffy

Technical Report No. Nonr-562(20)/33
Division of Engineering
Brown University
Providence 12, R. I.

April 1963

Sponsored by Dept. of the Navy
Office of Naval Research
Under Contract Nonr-562(20)
Task Order NR-064-424

The Behavior of Metals at Elevated Temperatures under Impact with a Bouncing Ball*

by

C-H. Mok and J. Duffy**

Abstract

This report describes an investigation into the behavior of metals under impact at elevated temperatures. In a series of tests, a hard spherical ball strikes the flat surface of a massive specimen, which in one instance was a commercially pure lead and in another an aluminum alloy. Tests were made at a number of temperatures at each of which the velocity of impact and the velocity of rebound were measured, as well as the size of the permanent indentation in the specimen surface, and the time of contact between ball and specimen. Through dimensional analysis, relations were derived which predict quite accurately the time of contact and the diameter of the permanent indentation for a given material. Following Tabor, energy was used to compute the dynamic yield pressure; and the present investigation offers a further understanding of this quantity. In addition the experimental results are in agreement with the work of both Raman and Davies, who showed that an extremely low impact velocity is needed for impact to be entirely elastic. Finally, present results indicate a possibility that impact tests can be used to measure the dynamic yield stress, but a more complete investigation of this question is reserved for a later report.

---

* The results in this paper were obtained in the course of research sponsored by the Office of Naval Research under Contract Nonr-562(20) with Brown University.

** Respectively Research Assistant and Associate Professor, Division of Engineering, Brown University, Providence, R. I.

I. Introduction.

In a common type of dynamic hardness test, a small but hard indenter is allowed to fall under the action of gravity onto a massive specimen. It is usual to measure the height of drop and either the height of rebound or the size of the indentation remaining in the specimen. Martel, for instance, defined "dynamic hardness number" as the ratio of the energy of the indenter immediately before impact to the volume of the indentation [1]*. This ratio has the units of a stress. Shore, on the other hand, used the height of rebound as a measure of hardness, keeping the height of drop constant [2]. Many other investigators have performed hardness tests of this type. One might mention the work of Raman [3], who measured the coefficient of restitution as a means of gaging the extent of elastic recovery over a range of impact velocities.

Although hardness tests by means of a bouncing ball are easy to perform, the difficulties arise in the interpretation of results. Whereas one can easily define dynamic hardness in terms of measurable quantities, it is considerably more difficult to relate these quantities to properties of the specimen material such as, for instance, the yield stress or the Young's modulus. To do this it would be necessary to have a detailed analysis of the impact process. It is evident, however, that this process is extremely complicated so that even the most thorough analyses as, for instance, those of Andrews [4,5,6] and of Tabor [7] are necessarily based upon

---

* Numbers in brackets refer to the bibliography at the end of the paper.

a number of assumptions. Andrews, in investigating the collision of two spheres of soft metal, assumes that the process includes three stages. The impact starts with an elastic deformation which obeys Hertzian theory. As soon as the yield pressure p_o is reached, a circular plastic region will form over which the pressure is constant and equal to p_o. This region enlarges under further forward motion of the spheres while the remaining outer annular region of the area of contact remains elastic. Finally, the spheres stop their approach and start moving apart under an elastic action of the entire deformed contact area. Tabor, in considering the problem of a comparatively hard ball striking a massive flat specimen, neglects the elastic action of the first two stages. On the basis of an energy analysis, he obtains a "mean yield pressure", P_d, for the plastic portion of the impact process and a mean pressure at the beginning of the elastic recovery stage, P_r. Experimentally, he found that the values of P_r are lower than those of P_d and closer to the yield pressure obtained in static hardness tests. Tabor argues that viscous effects in the specimen are responsible for this difference in the values of P_d and P_r. These two analyses, i.e. those of Andrews and Tabor, furnish the best available physical description of the impact process and one satisfactory from a qualitative point of view. The predicted values of time of contact during impact, of the diameter of the permanent indentation, and of the coefficient of restitution, while not in close quantitative agreement

with experimental results always tend in the right direction.

Crook [8] used a piezo-electric crystal to measure the total force throughout the duration of the impact process. He found that the pressure between the impacting bodies is very nearly constant up to the maximum force and that the magnitude of this pressure is nearly equal to that of Tabor's P_d. There is, in addition, further plastic deformation beyond the point of maximum force before the unloading of the specimen becomes entirely elastic. Crook maintains that the difference between the values of P_d and P_r cannot be due to viscous effects as was suggested by Tabor. His argument is that if the mean pressure between the bodies were dependent on the viscosity of the specimen then this pressure would have to vary with the rate of strain, whereas his tests indicate it remains substantially constant while the rate of strain starts at a high value and then goes decreasing. As further evidence, Crook cites the very careful tests of Davies [9], who found that the threshold of plastic deformation occurs at a very low impact velocity, but that even under these conditions in which viscous effects must be small, the pressure acting on the indenter is higher than the static yield pressure of the specimen material.

Raman [3] measured the coefficient of restitution in the impact between two small identical balls, each suspended as a pendulum. The materials tested were copper, aluminum and lead, all at room temperature. His results show an increase

in the value of the coefficient of restitution, e, as the impact velocity is decreased. Raman was able to decrease the impact velocity until it was just low enough for e to equal unity for copper and for aluminum. Practical limitations prevented measurements at lower velocities. For lead his highest value of e was about 0.80.

The present experiments were undertaken for two reasons: first, because the results of ball drop tests lie within a range of strain rates not easily covered using propagating waves and, secondly, because of the ease with which these tests can be performed whether the specimen be at room temperature or at an elevated temperature. Previous work at elevated temperatures using a dropping ball (e.g. Lea [10], Sauerwald and Knehans [11]) was concerned mainly with obtaining the dynamic hardness numbers of various materials. Our general plan was to investigate the ball drop test as such, and in particular, to see how results are affected by the temperature of the specimen. For this purpose the work of previous investigators was studied and, in some instances, extended. In addition, it was found that dimensional analysis leads to relations between the measured quantities which predict quite accurately experimental results. Finally, we wished to examine the possibility of using ball drop tests to obtain a more general understanding of the behavior of materials. Unfortunately, one is limited experimentally in this respect, in that for the materials tested it is almost impossible in a simple set-up to attain a low enough velocity for a purely

elastic impact [3,9]. On the other hand, there is apparently a possibility that the results can be interpreted so as to give values of the dynamic yield stress of the material at different strain rates. While referred to below, this last subject is in the main reserved for a later investigation.

II. Analysis of Impact Process.

(1) Coefficient of restitution.

The coefficient of restitution, e, can be defined as the ratio of the magnitude of rebound velocity to velocity of impact. For the bouncing ball tests the work of Hunter [12], of Rayleigh [13], and of Banerji [14] has shown that the amount of energy going into elastic waves within the solid, into vibrations of the indenting ball, or into sound waves, is small, so that nearly all the energy dissipated goes to the formation of a permanent indentation. As a result, the coefficient of restitution provides a qualitative description of the mechanical behavior of the material of the specimen, e.g. entirely elastic when $e = 1$, entirely inelastic when $e = 0$. A set of curves showing the dependence of the coefficient of restitution on impact velocity v_1 and on the temperature of the material is useful from this point of view. In particular, any sharp changes in the slope of the e-v_1 curve should reveal, in general, a transition from one dissipation mechanism to another or to elastic impact. It would be of interest, for instance, if one could compare lead at room temperature to

other metals at an elevated temperature by finding in both instances the transition from elastic to inelastic impact. Unfortunately this is not possible with the simple set-up used in the present tests because one can never achieve quite low enough velocities to obtain an entirely elastic impact.

(2) Tabor's analysis.

The assumption of elastic-perfectly plastic action in the impact process, i.e. flow with a constant dynamic yield pressure, seems justified on the basis of the results of Tabor's and Andrews' experiments. It is not clear, however, how one can calculate the magnitude of this yield pressure. The first investigator to study the problem was Martel [1], who suggested that the yield pressure be computed from the relation

$$P_d = \frac{W_1}{V_a} = \frac{mgh_1}{V_a} \qquad (1)$$

for a ball of diameter D dropped from a height h_1. In this expression W_1, m, and g denote respectively the total energy of impact, the mass of the ball, and the acceleration of gravity. V_a is the apparent volume of the permanent indentation, that is, the volume computed from the observed indentation diameter d and assuming that the radius of curvature of the indented surface is equal to that of the impacting ball. If r_1 and r_2 stand, respectively, for the radius of curvature of the ball and of the permanent

indentation, then

$$V_a = \frac{\pi a^4}{4r_1}$$

where $a = \frac{d}{2}$, whereas the actual volume of the indentation is nearer

$$V_r = \frac{\pi a^4}{4r_2}$$

It is evident, of course, that Martel does not make use of the energy of rebound. Furthermore, in computing the indentation volume he neglects the elastic recovery. As a result of this recovery, the radius of curvature of the indentation r_2 exceeds the radius of the ball, r_1. Tabor [7] suggests that the total energy loss and the actual volume of the permanent indentation be used in computing yield pressure, giving

$$P_d = \frac{W_1 - W_2}{V_r} = \frac{mg(h_1 - h_2)}{V_r}$$

where h_2 is the rebound height.

To relate r_2 to r_1, Tabor assumes that the rebound process takes place entirely elastically starting with a ball of radius r_1 in a spherical seat of radius r_2. Moreover, he takes P_d as the mean pressure at the instant when the two bodies have a maximum diameter of contact, $d = 2a$. Using Hertz' theory [15] to equate the elastic strain energy of the recovery process to the rebound velocity of the ball indenter,

he obtains

$$P_d = \frac{mg}{V_a}\left(h_1 - \frac{3}{8} h_2\right) \qquad (2)$$

which may be compared to Martel's relation (1) above. Clearly the difference between (1) and (2) depends on the height of rebound; and for small h_2 the results are not very different.

Alternatively, looking only at the rebound process, one finds for the mean yield pressure P_r on the basis of Hertz' theory [15]

$$P_r^2 = \frac{10}{3} \frac{mgh_2}{\pi^2 a^3} \Bigg/ \left[\frac{1-\nu_1^2}{E_1} + \frac{1-\nu_2^2}{E_2}\right] \qquad (3)$$

where E_1, ν_1 and E_2, ν_2 are, respectively, the Young's moduli and Poisson's ratios of ball and specimen.

Tabor compares values of P_d and of P_r computed on the basis of Equations (2) and (3), respectively, to the value of the static yield pressure P_s needed to produce an impression of the same diameter as in the corresponding impact test. He found first that P_s is always less than either P_r or P_d. Furthermore, P_r nearly always remains equal to about 1.1 P_s, whereas the ratio P_d/P_s, while always above 1.1, is greater the softer the metal. Tabor attributes this difference in the relative magnitude of P_d and P_r to the viscous effects present in the softer metals. Inelastic effects, whether time dependent or not, must occur almost exclusively during the loading process, i.e. as the ball is

moving down. Their presence, therefore, may influence the value of P_d. Rebound, however, is largely elastic; and rebound height is determined by the pressure between the ball and the specimen at the start of the rebound process. It can be expected that this pressure will depend almost entirely on the yield stress. Tabor's conclusion, therefore, is two-fold: first, that P_r will be always nearer P_s in magnitude, and second, that P_r will be influenced mainly by plastic (i.e. time-independent) effects as opposed to viscous effects. This means not only that the ratio P_d/P_r will always exceed unity, but that it will increase as viscous effects become more important. This conclusion was borne out by Tabor's results.

(3) Crook's measurement of the force during impact.

Crook [8] attached his specimen to a long lead bar suspended horizontally, with a piezo-electric crystal between the specimen and the bar. A freely swinging ball or cylinder was used as the hammer to produce impact. The relative approach of the hammer and the specimen during the impact process was calculated on the basis of the elementary theory of elastic waves in a long slender bar. At the same time Crook derived a relation between impact force, relative approach, and time of contact during impact in the following way: he presumed that the impact process starts with a rigid perfectly-plastic action, thus making the force between the two bodies during their approach proportional to the area of contact; that the

approach stops when the maximum impact force is reached; and that immediately thereafter the two bodies start to move apart elastically under an action obeying Hertz' theory. Crook's analysis provides relations between impact force, relative approach, and time of contact, which agree closely with experimental values. He concludes that the assumption of perfectly plastic action with a constant yield pressure holds closely up to the instant when the maximum force of impact is attained. The value of the mean pressure P_D occurring at the moment of the maximum impact force is very close to that of P_d predicted on the basis of Tabor's theory. As a result, the use of P_d for the mean pressure existing between bodies in collision seems justified. However, a comparison of theoretical and experimental curves of impact force against time reveals that further plastic flow exists even after the maximum impact force is reached and before elastic rebound occurs. Obviously, this final plastic flow does not occur under constant pressure. Therefore, Tabor's suggestion that viscous effects account for the difference between the values of P_d and P_r seems doubtful to Crook. He points out that the mean pressure between the colliding bodies remains nearly constant over a considerable portion of the impact process, i.e. does not vary with the strain rate, which is decreasing. Accordingly, P_d cannot be strongly sensitive to viscous effects. On the other hand it seems evident from Crook's results that Tabor's P_d provides an accurate prediction of the dynamic yield pressure; the meaning of P_r is perhaps less clear. The fact remains, however, that the ratio P_d/P_r increases for softer metals

and, as the present experiments show, is greater at higher temperatures. These results are consistent with Tabor's explanation based on time effects.

(4) Dimensional analysis.

In the hope of gaining greater insight into the impact process, dimensional analysis was employed and the results compared to experimental values.

For a small hard ball dropping on a massive specimen one can take as dependent variables the coefficient of restitution, e, the indentation diameter, d, and the impact time, t. These depend on the mass m and diameter D of the indenting ball, as well as on its impact velocity v_1. In addition, they depend on the properties of the specimen material, in particular on its Young's modulus E and on the yield stress. For the latter, one can use some nominal yield stress, e.g. the static yield stress σ_y. The fact that the yield stress, and perhaps even the Young's modulus, are influenced by other quantities, such as strain rate, is presumed taken into account by the inclusion of the impact velocity among the independent variables. There are, of course, other factors which influence results but for the purposes of dimensional analysis the number of variables was limited to the above. The temperature of the specimen is presumed to affect only the Young's modulus and the yield stress, but not otherwise to enter into the problem.

If one considers first the indentation diameter d together with all the above independent variables, it may be shown that there exist a total of three independent dimensionless products which can be formed with these variables, namely

$$\frac{d}{D} \; ; \quad \frac{m\, v_1^2}{E\, D^3} \; ; \quad \text{and} \quad \frac{\sigma_y}{E}$$

On the basis of experimental results, d is known to be proportional to v_1^{α} where α is constant, so that the relation between these products is

$$\frac{d}{D} = f_1 \left(\frac{\sigma_y}{E}\right) \left[\frac{m\, v_1^2}{E\, D^3}\right]^{\alpha/2} \tag{4}$$

where $f_1(\sigma_y/E)$ remains unknown.

A similar analysis can be made by considering the time of impact, t, along with the five independent variables to obtain the three dimensionless products

$$\frac{t^2\, DE}{m} \; ; \quad \frac{m\, v_1^2}{ED^3} \; ; \quad \text{and} \quad \frac{\sigma_y}{E}$$

Since t is proportional to v_1^{β} where β is another constant one forms

$$\left[\frac{t^2\, DE}{m}\right]^{1/2} = f_2 \left(\frac{\sigma_y}{E}\right) \left[\frac{m\, v_1^2}{ED^3}\right]^{\beta/2} \tag{5}$$

in which $f_2(\sigma_y/E)$ is unknown. As will be seen below in Sections V. (2), the Equations (4) and (5) are in agreement with the test results.

A similar relation can be established between the coefficient of restitution and the five independent variables. It was found, however, that this relation failed to fit completely the experimental data, although at high velocities it is true that e is proportional to v_1^{γ} where γ depends on the independent variables (other than v_1) and on temperature. One must conclude that other variables than those considered also influence the coefficient of restitution.

(5) Delay time of plastic deformation.

A number of investigators, in particular Clark and Wood [16], have observed a delay in the initiation of plastic deformation under rapid loading conditions. These observations were made for simple tension tests with a material possessing a relatively definite yield stress. The results indicate that the delay time depends on the level of the applied stress. It might seem, at first, that this phenomenon could also be studied by performing impact tests at very low velocities. However, Davies [9] found that an impact velocity of less than approximately 27 cm/sec is necessary for an entirely elastic impact in steel. This means that for steel the delay time is less than the contact time if the latter is greater than that produced by a 27 cm/sec impact velocity. With lead and aluminum it can be expected that some plastic deformation will occur at even lower velocities. The fact that a coefficient of restitution of unity could not be obtained for these two materials with the present set-up indicates that the delay time was

always less than the contact time for the stress levels encountered.

(6) Prediction of total time of contact between ball and specimen during impact.

The total time of contact between the ball and the specimen is of importance since it is needed in calculating strain rates and in estimating the delay time of plastic flow. This time of contact was measured experimentally; but it is also useful to arrive at an estimate through a simple analysis of the contact process.

The total time of contact t was estimated from the relation

$$t = t_p + t_e \tag{6}$$

where t_p and t_e were calculated as follows. The quantity t_p is the time necessary to decelerate the ball from the impact velocity v_1 to a velocity equal in magnitude to the rebound velocity v_2 but directed down. For this computation the ball was taken as rigid and the specimen as rigid-perfectly plastic with a yield pressure P_d given by Equation (2). An integration of the equation of motion for the ball gives

$$t_p = \sqrt{\frac{m}{2\pi r_1 P_d}} \cos^{-1} e \tag{7}$$

where e is the coefficient of restitution, and r_1 and m, respectively, the radius and mass of the ball. According to this equation t_p is zero for an elastic collision and is

equal to

$$\frac{\pi}{2}\sqrt{\frac{m}{2\pi r_1 P_d}}$$

for a completely inelastic one. This last expression was originally derived by Tabor for impact with a rigid-perfectly plastic specimen [7]. The remaining time of contact, t_e, is taken as twice the time of rebound, and rebound is presumed to start immediately after the ball reaches its maximum contact area with the specimen. In the rebound process the ball is forced to move away from the specimen by the elastic action of both ball and specimen. Finally, separation occurs at the velocity v_2 leaving a permanent indentation of radius r_2 greater than the radius of the ball r_1. According to Hertz

$$t_e = 2.86\, m^{2/5}\left[\frac{1-\nu_1^2}{E_1} + \frac{1-\nu_2^2}{E_2}\right]^{2/5}\left[\frac{1}{r_1} - \frac{1}{r_2}\right]^{1/5} v_2^{-1/5} \qquad (8)$$

In this expression $\left[\frac{1}{r_1} - \frac{1}{r_2}\right]$ can be calculated from the diameter of the permanent indentation d by

$$\frac{1}{r_1} - \frac{1}{r_2} = \frac{3\pi}{2}\frac{P_r}{d}\left[\frac{1-\nu_1^2}{E_1} + \frac{1-\nu_2^2}{E_2}\right]$$

where P_r is given by Equation (3). However, if no permanent indentation is left then, according to Equation (7), t_p vanishes, and hence the total time of contact is given by Equation (8) with $1/r_2$ equal to zero and with $v_2 = v_1$.

III. Technique used in Present Experiments.

In the present tests, bearing balls were dropped on a cylindrical specimen shaped as shown in Figure 1. Solid steel balls of 1" and 1/2" diameter were used, as well as 2017 aluminum alloy balls of 1" diameter either solid or lead-filled. The lead-filled balls were made by drilling a 1/2" hole through the center of the ball and filling it with lead. The specimens on which the balls were dropped were 10" long and 6" in diameter. They were made of either of two materials: commercially pure lead and an aluminum alloy (6061-T6). Specimens of the latter material were tested both in the as-rolled condition and also after annealing at 900°F for 3 hours. The serrations cut into the outer surface and the inclinations of these surfaces were intended to minimize the effect on the impact process of reflected waves. Care was taken that the specimen's top surface, on which the ball impinged, was always a freshly machined surface. In addition, the balls were dropped only in the neighborhood of the center of this surface at points relatively far apart from one another.

For the tests at elevated temperatures, the specimens were heated by placing them within a cylindrical oven provided with a cover which could be opened and closed rapidly for each test. The temperature distribution was measured by means of thermocouples imbedded at various points throughout the specimen, thus ensuring uniformity of temperature over the testing surface and beneath it.

Two techniques were used in the tests. For high velocities of impact (> 200 cm/sec) the ball was allowed to drop freely onto the horizontal surface of the specimen. For velocities less than 200 cm/sec, the ball was suspended by four fine threads and allowed to swing as a pendulum striking the specimen which now was placed with its axis horizontal.

In the free fall experiments the ball was held in place above the specimen by means of a small electromagnet. It was released by throwing a switch which reversed the electric current in the coil to just such an extent as to overcome the residual magnetism. To avoid giving the ball an angular impulse on releasing it the tip of the magnetic core from which it hung was spherical so contact was at only one point. Impact velocity was calculated simply from the height of drop, h_1. Rebound velocity, similarly, was found from the rebound height, h_2, as determined photographically (see for example Figure 2). In order to prevent the ball from striking twice in the same spot, the surface of the specimen was tilted at about 1° from the horizontal. This made it easier also to determine accurately the height of rebound. The coefficient of restitution, e, defined as the ratio of rebound velocity to impact velocity was evaluated using the relation

$$e = \frac{h_2}{h_1}$$

Measurements also were made of the time of impact. For these

tests a fine constantan wire (D = .003") was attached to the ball and the time of electrical contact between ball and specimen was measured by means of a high speed electronic counter.

In the low velocity impact tests, the ball was suspended in a four-threaded pendulum about 184 cm. long. It was held between two thin aluminum plates to which the threads were attached (Figure 3). Care was taken that the center of mass of the ball lie on a line with the directions of the threads and also that the impact occur at the lowest point in the path of travel of the ball. The release for the ball consisted simply of a very short silk thread held between knife edges which were parted suddenly. Measurements of time of impact were made with the same technique as in the free fall test, whereas the impact and rebound velocities were found from the rate at which the ball in its travel interrupted a thin horizontal slit of light. This latter measurement involved the use of a photocell and an oscilloscope. Figure 4 shows a typical photograph.

IV. Presentation of Results.

The test results are presented in Tables 1-9. The time of contact during impact, t, is a measured quantity; the indentation diameter, d, is an average of four measurements made with a microscope. When the impact velocity is under 200 cm/sec. the velocity of impact and the coefficient of restitution, e, are measured quantities. For tests above 200 cm/sec. measured

quantities are height of drop h_1 and height of rebound h_2 from which the velocity of impact and the coefficient of restitution are calculated.

Results with different indenters are similar in nature so that they need not all be presented graphically. Figures 5-9 show the variation of e, t and d with impact velocity v_1 for a 1" steel ball striking in turn specimens of lead, annealed aluminum and as-rolled aluminum. One observes that as the velocity decreases the coefficient of restitution and the time of impact increase, while the size of the indentation decreases. Results of this kind have already been obtained by others [3,6] and indicate, among other things, that the impact process is more nearly elastic at lower velocities. An increase in temperature presumably decreases both the yield stress and the Young's modulus of the material and, hence decreases the coefficient of restitution and increases the impact area. The influence of temperature on time of contact is harder to predict. According to Tabor, in a rigid-perfectly plastic impact an increase in temperature increases the contact time. This conclusion is in qualitative agreement with present results which, however, show some scatter particularly at lower velocities.

The changes in the measured quantities for lead and the annealed aluminum alloy with temperature seem small if one remembers that the melting points for these materials are respectively 621°F and 1200°F (Figures 5-7). A relatively

temperatures (Figures 10-15). Since d/D differs from test to test, its value is indicated next to each point in question. All results seem to fall on one curve, with a minimum of scatter, irrespective of the size or material of the indenting ball. However, the curve shows not only the dependence of P_d on strain rate (d/tD) but also its dependence on strain (d/D), since the value of d/D varies along the curve and tends to decrease at lower strain rates. (A plot of results showing P_d versus d/D illustrates this point more clearly.) In Figures 10-15 the intercept with the vertical axis gives the value of P_d corresponding to zero strain rate at a small strain. This value of P_d can be interpreted in terms of the static yield stress through the relation

$$\sigma_y = \frac{P_d}{2.8}$$

which was derived empirically by Tabor [7] on the basis of static tests and which also has received some theoretical confirmation from the work of Ishlinsky [17] and from the analyses of the punch problem by Hencky [18] and by Shield and Drucker [19]. Table 11 shows a comparison between values of yield stress so obtained and the virgin yield of the material as measured in a simple compression test. Agreement is good in all cases except for the annealed aluminum alloy at 900°F. This result suggests the possibility that P_d can by proper interpretation give a measure of the dynamic yield stress of the material at a given strain and a given strain rate. Work along these lines is continuing.

(2) Results based on dimensional analysis.

Equation (4), derived above on the basis of dimensional analysis, may be repeated here for convenience:

$$\frac{d}{D} = f_1 \left(\frac{\sigma_Y}{E}\right) \left[\frac{m\, v_1^2}{ED^3}\right]^{\alpha/2} \qquad (4)$$

Measurements of the indentation diameter at various impact velocities indicate that α is approximately 0.45. The fact that d depends on v_1^{α} had already been found by Schneider [20] and others for materials at room temperature, and present results indicate that this holds irrespective of temperature for lead and aluminum (Figure 16). It appears also that the numerical value of α does not depend on the size or material of the indenting ball and only slightly on specimen material (Table 12).

The validity of Equation (4) was examined experimentally by varying one at a time the parameters in the equation. The ball diameter, D, was the first to be changed. Specimens were tested with balls of different diameters at a number of temperatures and impact velocities. Next, the dependence on the mass m of the ball was examined by changing the material of the indenter, first from steel to aluminum and then from solid aluminum to lead-filled aluminum. In each case the tests were run at a number of temperatures and impact velocities. The results consistently show strong agreement with values predicted on the basis of Equation (4), which thus appears of value in predicting the indentation diameter in impact tests.

One must add that the function $f_1(\sigma_y/E)$ remains undetermined, although according to Table 12, its numerical value does not depart greatly from 4.5.

Dimensional analysis also gives an equation for the total time of impact, namely

$$\left[\frac{t^2 DE}{m}\right]^{1/2} = f_2\left(\frac{\sigma_y}{E}\right)\left[\frac{m v_1^2}{ED^3}\right]^{\beta/2} \qquad (5)$$

according to which t is proportional to v_1^{β} where β is a new constant. This relation is in agreement with the present results for which $\beta \approx -0.15$, irrespective of temperature, indenter material or specimen material. However, rather than presenting a graph showing the variation of t with v_1, it is more interesting to make use of Equation (4) as well and instead plot d/t against v_1. Typical values are shown in Figure 17. It may be noted that for each material and using one indenter all points fall on one line no matter what the temperature. The dependence of t on D and on m was examined by varying each of these parameters independently. Results show strong agreement with predications based on Equation (5). The values of $f_2(\sigma_y/E)$ given in Table 12 are near 5, but the variation in $f_2(\sigma_y/E)$ is greater than that of $f_1(\sigma_y/E)$.

One should note how closely the above results, which are based on dimensional analysis, compare to results based on a simple physical analysis of the impact process. For

instance, for elastic impact Hertz' theory yields

$$d = 1.5 \left\{ \left[\frac{1-\nu_1^2}{E_1} + \frac{1-\nu_2^2}{E_2} \right] D^2 m^2 v_1^2 \right\}^{1/5}$$

$$t = 3.29 \left\{ \left[\frac{1-\nu_1^2}{E_1} + \frac{1-\nu_2^2}{E_2} \right]^2 m^2 \Big/ D v_1 \right\}^{1/5}$$

which corresponds to $\alpha = 0.40$ and $\beta \approx -0.20$. At the other extreme, for rigid-perfectly plastic impact, according to Tabor's analysis,

$$d = 2 \left(\frac{Dm}{\pi P} \right)^{1/4} v_1^{1/2}$$

$$t = \frac{\pi}{2} \sqrt{\frac{m}{\pi P D}}$$

yielding values of $\alpha = 0.50$ and $\beta = 0$. It is interesting to note that experimental values of α and β lie, respectively, between the two values predicted by these simple analyses. (Actually, the experimental values of α and β vary somewhat with impact velocity tending more toward the perfectly plastic values as the impact velocity is increased.) Equations (4) and (5) predict values of d and t which agree quite closely with experimental results for either lead or the aluminum alloy at any temperature. This would seem to indicate that viscous effects, if present, influence the impact process mainly through the properties of the materials, i.e. through the functions $f_1(\sigma_y/E)$ and $f_2(\sigma_y/E)$.

(3) Approximation for the total time of impact.

Approximate values of the total time of impact were calculated on the basis of Equation (6) using the present test results. In the calculations P_d and P_r are given, respectively, by Equations (2) and (3). The values of E_1 and E_2 are taken from Table 13 and Poisson's ratio was set equal to 0.3 for both ball and specimen. Figures 18 and 19 show typical results. In general, the difference between calculated and experimental values is less than 10% for lead and 15% for aluminum over the entire range of velocities. Apparently, therefore, Equation (6) gives a good estimate of the total time of impact for this velocity range.

(4) The yield pressure as evaluated by P_r or P_d; meaning of P_d/P_r.

One important result of the hardness test is a measure of yield pressure. As mentioned in section II.(2) and depending on the analysis, Tabor obtains two different expressions for yield pressure, viz. P_d and P_r. It is of interest to contrast these two quantities to see which gives more reliable information on the yield properties of the specimen. Such a comparison already was made both by Tabor [7] and by Crook [8]. However, some additional comments based on present results may be of value.

Equation (3) gives the quantity P_r as derived by Tabor from the rebound height. Since it is based on Hertz' theory

of elastic contact, P_r will be sensitive to the properties of both the indenter and the specimen. Experimental results confirm this sensitivity to indenter properties (Table 14). Therefore, comparisons of test results obtained with different types of indenters cannot be made directly.

In contrast, P_d is obtained by equating the loss in kinetic energy to the energy required to produce the indentation. It appears from present results, as given in section V.(1) that P_d is largely independent of the properties of the indenter, i.e. depends almost exclusively on the specimen properties. Moreover, in Crook's experiments the value of P_d was close to the value of the mean yield pressure at the moment when the impact force reaches its maximum value as given by direct measurement of impact force. It would thus seem that P_d furnishes a more reliable measure of specimen properties than does P_r.

According to Tabor's explanation, P_r gives the magnitude of the yield pressure at the end of plastic action (i.e. at the start of elastic recovery) and P_d gives the average value of the yield pressure for the entire plastic process. Tabor argues that when viscous effects are present, P_d will be greater than P_r because the strain rates are greater during the plastic process than they are at the start of elastic recovery. Consequently, the ratio P_d/P_r has a value greater than unity and a higher value for softer materials. Present results do not make Tabor's explanation any less valid. The

ratio P_d/P_r was found greater than unity in all cases. (The one exception is for tests at low velocities with a 1" lead filled 2017 aluminum alloy ball. In this case the high values of P_r may well be explained by the dependence of P_r on the properties of the indenter, i.e. on the spring-like action of the aluminum surrounding the lead core). The present experiments also show that P_d/P_r is higher for specimens of lead than for those of aluminum alloy and, moreover, is greater the higher the temperature.

(5) The influence of temperature.

As expected, for the same impact velocity the coefficient of restitution, e, decreases with an increase in temperature (e.g. Fig. 5 and Table 1). This is apparently due in part to a decrease in both the Young's modulus and the yield pressure of the material, as evidenced by the drop in the values of P_d and P_r. In addition, the ratio P_d/P_r is greater at more elevated temperature. This is in line with Tabor's theory since an increase in temperature undoubtedly produces an increase in the viscosity of the materials.

The fact that the values of P_d, e and P_d/P_r for an annealed aluminum alloy specimen at high temperature tend to those of lead at room temperature (Figures 10-15, 5,6, Table 15) would seem to suggest that by choosing an appropriate temperature the two materials will have a similar behavior. However, for the temperature range covered in these experiments

(70° to 900°F for annealed aluminum alloy, 70°F to 450°F for lead) the corresponding changes in the properties of the two materials are small in comparison to the difference in their properties at room temperature. This is in spite of the fact that the above temperature ranges are quite large (the melting points of the materials are respectively about 1200°F and 600°F).

Conclusions

The principal conclusions one can draw on the basis of this investigation bear more directly on the impact test as such than on the general behavior of materials. For the bouncing ball test, dimensional analysis yields two relations namely

$$\frac{d}{D} = f_1\left(\frac{\sigma_y}{E}\right)\left[\frac{m\, v_1^2}{E\, D^3}\right]^{\alpha/2}$$

and

$$\left[\frac{t^2_{DF}}{m}\right]^{1/2} = f_2\left(\frac{\sigma_y}{E}\right)\left[\frac{m\, v_1^2}{E\, D^3}\right]^{\beta/2}$$

which predict quite accurately for any temperature the dependence of the indentation diameter and the time of contact during impact on the mass, diameter, and velocity of the ball. Experimental results indicate that $\alpha \approx 0.45$ and $\beta \approx -0.15$. These values compare to $\alpha = 0.40$ and $\beta = -0.20$ obtained from a simple analysis assuming elastic impact, and to $\alpha = 0.50$ and $\beta = 0$ for a perfectly plastic impact. Furthermore, although the experimental values of α and β are not very sensitive

to changes in impact velocity they do tend toward the elastic values as the velocity is decreased.

On the other hand, the results of dimensional analysis give no clue to the form of the functions $f_1(\sigma_y/E)$ and $f_2(\sigma_y/E)$ except that numerical values of these functions vary little with temperature.

In regard to Tabor's expressions P_d and P_r for the dynamic yield pressure, our results do not contradict Tabor's understanding of these quantities. On the basis of his experiments using specimens of different materials, Tabor concluded that the ratio P_d/P_r is greater for those materials whose stress-strain relation is more strongly time dependent. Present results appear to be consistent with this conclusion, in that, for a given material, this ratio is greater at higher temperatures where one would expect viscous effects to be more pronounced. Our results also show that for any given material the value of P_d changes with impact velocity presumably varying with the strain and the strain rate. This result does not agree with the supposition made by previous investigators that P_d remains constant throughout the impact process. It is, however, not inconsistent with Tabor's interpretation of the ratio P_d/P_r.

The total time of contact during impact was measured for the lead and aluminum specimens at different temperatures. The results are presented in the text and compare closely to

values derived on the basis of the simple analysis of the contact process presented in section II.(6) above.

Results of impact tests using a bouncing ball are difficult to interpret in terms applicable to a more general understanding of the behavior of materials. However, it appears that the static yield stress can be obtained by an extrapolation of present results involving the dynamic yield pressure P_d to a zero strain rate. This suggests the possibility that the dynamic yield stress at various strain rates can also be measured with a bouncing ball; work in this direction is continuing.

One can look at the results also by plotting the coefficient of restitution against impact velocity. As expected, this coefficient increases at lower velocities where a greater proportion of the kinetic energy of impact is recovered. It might be supposed that for values of the velocity beneath a certain critical value, the coefficient of restitution would equal unity. This critical velocity could then be used as a measure of the limit of elastic action and, perhaps, as a reference point which would allow comparisons between the behavior of different metals at different temperatures. Unfortunately, as both Davies and Raman found already, the critical velocity is so low that it barely can be attained in a simple experiment even at room temperature.

Bibliography

1. Martel, "Sur la Mesure de la Dureté des Métaux," Commission des Méthodes d'Essai des Materiaux de Construction, Paris, Vol. iii, Section A (Métaux), 1895, pp. 261-277.

2. Shore, A. F., "Report on Hardness Testing: Relation between Ball Hardness and Scleroscope Hardness," J. Iron and Steel Inst., No. 2, 1918, p. 59.

3. Raman, C. V., "The Photographic Study of Impact at Minimal Velocities," Phys. Review, Vol. 12, 1918, pp. 442-447.

4. Andrews, J. P., "Theory of Collision of Spheres of Soft Metals," Phil. Mag., Vol. 9, 7th Series, 1930, p. 593.

5. Andrews, J. P., "On the Impact of Spheres of Soft Metals," Phil. Mag., Vol. 8, 7th Series, 1929, p. 781.

6. Andrews, J. P., "Experiments on Impact," Proc. Phys. Soc. of London, Vol. 43, 1931, p. 8.

7. Tabor, D., The Hardness of Metals, Oxford, 1951.

8. Crook, A. W., "A Study of Some Impacts between Metal Bodies by a Piezo-electric Method," Proc. Royal Soc. of London, Series A, Vol. 212, 1952, p. 377.

9. Davies, R. M., "The Determination of Static and Dynamic Yield Stresses Using a Steel Ball," Proc. Royal Soc. of London, Series A, Vol. 197, 1949, p. 416.

10. Lea, F. C., Hardness of Metal, Charles Griffin & Co., Ltd., London, 1936.

11. Von Sauerwald, F., Knehans, K., "Über die Temperaturabhängigkeit der Härte, die als spez. Verdrängungsarbeit definiert ist, bei Metallen," Zeit, für anorganische und allgemeine Chemie, Vol. 140, 1924, p. 227.

12. Hunter, S. C., "Energy absorbed by Elastic Waves during Impact," J. Mech. Phys. Solids, Vol. 5, 1957, p. 162.

13. Rayleigh, Lord, "On the Production of Vibrations by Forces of Relatively Long Duration, with Application to the Theory of Collisions," Phil. Mag., Vol. 11, 1906, 6th Series, p. 283.

14. Banerji, S., "On Aerial Waves generated by Impact," Phil. Mag., Vol. 32, 1916, 6th Series, p. 96, and Vol. 35, 1918, 6th Series, p. 97.

Bibliography (Cont.)

15. Hertz, H., Miscellaneous Papers, 1896, London, p. 161.

16. Clark, D. S. and Wood, D. S., "The Time Delay for the Initiation of Plastic Deformation at Rapidly Applied Constant Stress," Proc. ASTM, Vol. 49, 1949, p. 717.

17. Ishlinsky, A. Iu., "The Problem of Plasticity with Axial Symmetry and Brinell's Test," Prikladnaia Matematika i Mekhanika, Vol. 8, 1944, pp. 201-224.

18. Hencky, H., "Uber einige statisch bestimmte Fälle des Gleichgewichts in plastischen Körpern," Zeit. ang. Math. Mech., Vol. 3, 1923, pp. 241-251.

19. Shield, R. T. and Drucker, D. C., "The Application of Limit Analysis to Punch-indentation Problems," J. Appl. Mech., Vol. 20, 1953, pp. 453-460.

20. Schneider, J. J., "Die Kugelfallprobe," Zeit. des Vereines deutscher Ingenieure, Vol. 54, 1910, p. 1631.

TABLE 1

Results obtained with 1" Steel Ball striking Lead Specimen

Impact Velocity v_1 (cm/sec)	Impact Height h_1 (cm)	Rebound Height h_2 (cm)	Coeff. of Restitution e	Impact Time, t (10^{-4} sec)	Indentation Diameter d (cm)
Room Temperature					
3.5			0.24	6.62	0.088
13.9			0.21	4.08	0.156
26.2			0.186	3.85	0.213
54			0.169	3.44	0.296
91.7			0.144	3.54	0.388
102			0.142	(10.14)	0.380
221	25.0	0.31	0.111	--	0.531
221	25.0	0.40	0.126	2.94	0.530
313	50.0	0.68	0.117	2.88	0.622
443	100.2	1.14	0.107	--	0.720
443	100.2	1.17	0.108	2.74	0.728
523	139.6	1.53	0.105	2.77	0.794
Temperature = 300°F					
3.7			0.239	6.39	0.093
10.7			0.193	4.95	0.151
21.0			0.178	4.46	0.207
54.0			0.165	3.99	0.292
98.5			0.142	3.60	0.399
225	25.8	--	--	3.17	0.586
225	25.8	0.35	0.116	3.17	0.573
315	50.5	0.54	0.103	3.06	0.658
443	100.1	0.90	0.095	2.93	0.784
523	139.6	1.15	0.091	2.92	0.835
Temperature = 450°F					
2.3			0.268	6.52	0.116
11.2			0.198	4.85	0.155
53.4			0.132	3.83	0.309
99.6			0.132	3.51	0.410
221	25.0	--	--	--	0.585
313	50.0	0.44	0.094	3.31	0.674
441	99.4	0.70	0.084	3.04	0.789
524	140	0.83	0.077	2.94	0.858

TABLE 2

Results obtained with 1" Steel Ball

Striking Annealed Specimen of 6061-T6 Aluminum

Impact Velocity v_1 (cm/sec)	Impact Height h_1 (cm)	Rebound Height h_2 (cm)	Coeff. of Restitution e	Impact Time, t (10^{-4} sec)	Indentation Diameter d (cm)
Room Temperature					
2.1			0.665	3.28	--
12.5			0.563	2.44	0.091
29.9			0.490	1.74	0.135
54.9			0.383	1.55	0.178
94.6			0.328	1.45	0.231
220	24.7	2.52	0.319	1.24	0.336
220	24.7	2.42	0.313	--	0.344
220	24.7	2.37	0.310	1.27	0.340
313	50.1	4.38	0.296	--	0.406
313	50.1	4.47	0.299	(2.10)	0.402
313	50.1	4.30	0.293	(2.00)	0.405
313	50.1	4.24	0.291	1.22	0.403
443	100.3	7.82	0.299	1.18	0.470
524	140	9.05	0.254	(1.33)	0.514
524	140	9.00	0.254	1.20	0.521
Temperature = 400°F					
2.3			0.748	--	--
2.6			0.633	3.05	--
13.2			0.496	2.01	0.096
24.9			0.481	1.86	0.129
59.1			0.362	1.61	0.192
92.8			0.297	1.52	0.240
221	25.0	2.02	0.284	--	0.362
221	25.0	2.07	0.288	1.36	0.359
313	50.0	3.58	0.268	--	0.419
317	51.2	3.67	0.268	--	0.428
314	50.4	3.40	0.260	(1.38)	0.432
443	100.0	6.00	0.245	1.28	0.502
524	140.0	7.75	0.235	1.25	0.546
Temperature = 900°F					
2.1			0.566	3.62	--
14.6			0.424	2.27	0.110
28.7			0.376	1.97	0.152
51.8			0.300	1.84	0.200
95.1			0.259	1.62	0.262
213	23.1	1.35	0.242	--	0.379
313	50.1	2.40	0.219	--	0.456
313	50.1	2.53	0.225	--	0.454
316	51.0	2.52	0.222	1.40	0.455
443	100.2	4.15	0.204	1.38	0.536
524	140.1	5.27	0.194	1.32	0.583

TABLE 3

Results obtained with 1" Steel Ball striking As-rolled Specimen of 6061-T6 Aluminum

Impact Velocity v_1 (cm/sec)	Coeff. of Restitution e	Impact Time, t (10^{-4} sec)	Indentation Diameter d(cm)
Room Temperature			
3.01	0.981	2.56	--
3.48	0.980	2.52	--
30.8	0.834	1.49	0.096
91.3	0.689	1.21	0.166
Temperature = 400°F			
3.16	0.943	2.73	(-----)
25.3	0.807	1.68	0.086
96.1	0.543	1.28	0.186
Temperature = 900°F			
3.11	0.609	2.81	0.056
21.8	0.422	2.41	0.133
93.4	0.306	1.59	0.252

TABLE 4

Results obtained with 1/2" Steel Ball striking Lead Specimen

Impact Velocity v_1 (cm/sec)	Impact Height h_1 (cm)	Rebound Height h_2 (cm)	Coeff. of Restitution e	Impact Time, t (10^{-4} sec)	Indentation Diameter d (cm)
Room Temperature					
2.67			0.272	3.66	0.037
30.2			0.182	2.00	0.115
105			(0.087)	1.75	0.194
221	25	0.39	0.125	--	0.264
313	50	0.79	0.126	1.40	0.308
313	50	0.70	0.118	--	0.313
313	50	0.70	0.118	--	0.313
524	140	1.70	0.11	1.37	0.390
Temperature = 300°F					
2.89			0.264	3.65	0.042
22.3			0.217	2.22	0.106
98.1			0.146	(2.69)	0.205
312	49.8	0.58	0.108	--	0.329
443	100	1.0	0.100	1.61	0.383
524	139.8	1.27	0.095	1.44	0.416

TABLE 5

Results obtained with 1/2" Steel Ball striking Annealed Specimen 6061-T6 Aluminum

Impact Velocity v_1 (cm/sec)	Impact Height h_1 (cm)	Rebound Height h_2 (cm)	Coeff. of Restitution e	Impact Time, t (10^{-4} sec)	Indentation Diameter d (cm)
Room Temperature					
2.01			0.717	1.58	--
30.2			0.426	0.89	0.071
94.7			0.41	0.72	0.118
221	25	3.1	0.352	--	0.160
313	50	5.85	0.342	0.59	0.194
443	100	10.45	0.324	0.56	0.227
524	140	13.2	0.307	0.55	0.248
524	140	12.8	0.302	--	0.250
Temperature = 400°F					
2.18			0.662	1.74	--
31.5			0.367	0.94	0.071
97.4			0.342	0.70	0.124
221	25	2.55	0.319	--	0.176
312	49.8	4.69	0.307	0.62	0.201
443	99.9	8.7	0.294	0.60	0.244
524	140.4	10.50	0.273	0.58	0.266

TABLE 6

Results obtained with 1" 2017 Aluminum Ball striking Lead Specimen

Impact Velocity v_1 (cm/sec)	Coeff. of Restitution e	Impact Time, t (10^{-4} sec)	Indentation Diameter d(cm)
Room Temperature			
2.05	0.491	5.98	0.051
12.7	0.379	2.80	0.113
28.2	0.269	2.57	0.166
46.3	0.234	2.24	0.216
92.8	0.154	1.92	0.285
Temperature = 300°F			
2.87	0.308	5.00	--
12.8	0.288	2.90	0.129
25.8	0.216	2.70	0.176
46.4	0.193	--	0.232
89.5	0.073	2.62	0.311
Temperature = 450°F			
3.62	0.210	4.90	0.071
13.2	0.210	3.25	0.132
29.0	0.193	2.90	0.185
44.4	0.173	2.51	0.226
92.2	0.124	2.20	0.315

TABLE 7

Results obtained with 1" 2017 Aluminum

Ball striking Annealed Specimen of 6061-T6 Aluminum

Impact Velocity v_1 (cm/sec)	Coeff. of Restitution e	Impact Time, t (10^{-4} sec)	Indentation Diameter d(cm)
Room Temperature			
2.64	0.791	2.28	--
13.5	0.696	1.48	0.069
24.1	0.652	1.31	0.101
42.6	0.495	1.16	0.125
93.5	0.436	0.98	0.176
Temperature = 400°F			
11.7	0.701	1.65	0.073
24.3	0.591	1.28	0.102
43.1	0.471	1.14	0.133
90.6	0.335	1.01	0.186
Temperature = 900°F			
47.8	0.411	1.20	0.134
93.0	--	1.12	0.194

TABLE 8

Results obtained with 1" 2017 Aluminum

Lead Filled Ball striking Lead Specimen

Impact Velocity v_1 (cm/sec)	Coeff. of Restitution e	Impact time, t (10^{-4} sec)	Indentation Diameter d (cm)
Room Temperature			
2.32	0.469	5.44	0.066
12.0	0.408	3.56	0.132
30.8	0.284	3.09	0.193
45.6	0.292	2.96	0.252
96.3	0.239	2.69	0.348
Temperature = 300°F			
3.26	0.270	6.59	0.079
10.9	0.263	--	0.147
27.2	0.259	3.54	0.210
48.4	0.240	3.31	0.269
90	0.230	3.14	0.364
Temperature = 450°F			
3.58	0.235	4.73	--
11.7	0.234	3.92	0.144
26.2	0.217	3.81	0.213
46.8	0.219	3.41	0.271
93.0	0.211	3.06	0.373

TABLE 9

Results obtained with 1" 2017 Aluminum Lead Filled Ball striking Annealed Specimen of 6061-T6 Aluminum

Impact Velocity v_1 (cm/sec)	Coeff. of Restitution e	Impact Time, t (10^{-4} sec)	Indentation Diameter d(cm)
Room Temperature			
2.16	0.872	3.25	--
11.2	0.726	1.81	0.081
27.3	0.696	1.64	0.113
40.3	0.595	1.50	0.141
93.5	0.63	1.31	0.208
Temperature = 400°F			
2.97	0.780	2.58	--
11.8	0.700	1.98	0.083
26.0	0.671	1.68	0.119
46.1	0.607	1.51	0.154
92.8	0.562	1.34	0.213
Temperature = 900°F			
13.0	0.684	2.02	0.094
46.8	0.565	1.65	0.167
93.0	--	1.50	0.232

TABLE 10

Dependence of P_d on d/tD

Material	Temp.	Indenting Ball	d/D	d/tD (sec^{-1})	P_d (kg/mm^2)
Lead	70°F	1" steel	0.313	1130	5.76
		½" steel	0.307	2240	6.18
	300°F	1" steel	0.329	1125	4.71
		½" steel	0.328	2280	5.01
Annealed 6061-T6 Aluminum	70°F	1" steel	0.205	1720	30.4
		½" steel	0.196	3550	38.3
	400°F	1" steel	0.215	1720	25.2
		½" steel	0.210	3600	28.9

TABLE 11

Static Yield Stress

(This table compares values of the static yield stress as obtained through an extrapolation of present impact test results to values found in simple compression and simple tension tests.)

Specimen: Lead

Source	70°F	300°F	450°F
Present Impact Tests	800 psi	710 psi	650 psi
Static Compression Test (0.2% Offset)	850 psi		

Specimen: Annealed 6061-T6 Aluminum

Source	70°F	400°F	900°F
Present Impact Tests	8,500 psi	7,000 psi	3,400 psi
Static Tension Tests* (0.2% Offset)	8,000 psi	6,500 psi	less than 2,000 psi

Specimen: As-rolled 6061-T6 Aluminum

Source	70°F	400°F	900°F
Present Impact Tests	36,000 psi	28,000 psi	3,000 psi
Static Tension Tests* (0.2% Offset)	40,000 psi	29,000 psi	less than 3,000 psi

* Data furnished by Alcoa Research Laboratory.

TABLE 12

Values of α, β, $f_1(\sigma_y/E)$, $f_2(\sigma_y/E)$

Indenting Ball	α			β			$f_1(\sigma_y/E)$ *			$f_2(\sigma_y/E)$ *		
	Lead Specimen											
	70°F	300°F	450°F	70°F	300°F	450°F	70°F	300°F	450°F	70°F	300°F	450°F
1" steel	0.44	0.45	0.45	-0.14	-0.13	-0.13	4.1	4.5	4.6	9.0	9.2	9.1
½" steel	0.44	0.44		-0.15	-0.15		4.0	4.0		7.8	7.9	
1" 2017 Aluminum	0.46	0.46	0.46	-0.18	-0.18	-0.18	4.7	5.0	4.8	5.6	5.5	5.5
1" 2017 Aluminum Lead Filled	0.46	0.45	0.46	-0.18	-0.19	-0.19	4.8	4.6	5.0	5.7	5.2	5.3
	Annealed 6061-T6 Aluminum Specimen											
	70°F	400°F	900°F	70°F	400°F	900°F	70°F	400°F	900°F	70°F	400°F	900°F
1" steel	0.47	0.47	0.46	-0.13	-0.13	-0.14	4.5	4.5	4.4	7.7	7.7	5.6
½" steel	0.47	0.47		-0.15	-0.15		4.5	4.5		6.1	6.1	
1" 2017 Aluminum	0.47	0.45	0.46	-0.17	-0.19	-0.19	4.1	3.8	3.6	5.5	4.5	4.5
1" 2017 Aluminum Lead Filled	0.46	0.45	0.46	-0.17	-0.18	-0.17	4.1	3.7	3.8	5.7	5.6	4.6

* Computed with Young's Moduli given in Table 13.

TABLE 13

Values of Young's Moduli (10^{11} dynes/cm^2)

used in Calculations

Temperature / Material	70°F	300°F	400°F	450°F	900°F
Lead*	1.6	1.3		1.2	
6061 Aluminum**	7.0		6.0		2.9
Steel	20				

* "Mechanical Properties of Metals at Low Temperatures," U.S. Dept. of Commerce, National Bureau of Standards, Circular 520, 1952, p. 4.

** Alcoa Research Laboratory.

TABLE 14

Dependence of P_r on Indenter Properties

(Room Temperature Tests)

Specimen	$\frac{d}{D}$	P_r			
		1" steel ball	½" steel ball	1" 2017 aluminum ball	1" 2017 alum. lead filled ball
Lead	0.11	3.2×10^3 psi	3×10^3 psi	3.1×10^3 psi	4.8×10^3 psi
Annealed 6061-T6 aluminum	0.07	29×10^3 psi	28×10^3 psi	30×10^3 psi	44×10^3 psi

In computing values of P_r, $\nu_1 = \nu_2 = 0.3$, while E_1 and E_2 are taken from Table 13.

TABLE 15

Dependence of P_d/P_r on Temperature

(Indenter: 1" Steel Ball)

Specimen	$\frac{d}{tD}$ (sec^{-1})	$\frac{d}{D}$	P_d/P_r				
			70°F	300°F	400°F	450°F	900°F
Lead	1120	0.31	2.0	2.23		2.38	
Annealed 6061-T6 Aluminum	1700	0.23	1.24		1.28		1.72
As-rolled 6061-T6 Aluminum	550	0.08	1.17		1.37		1.63

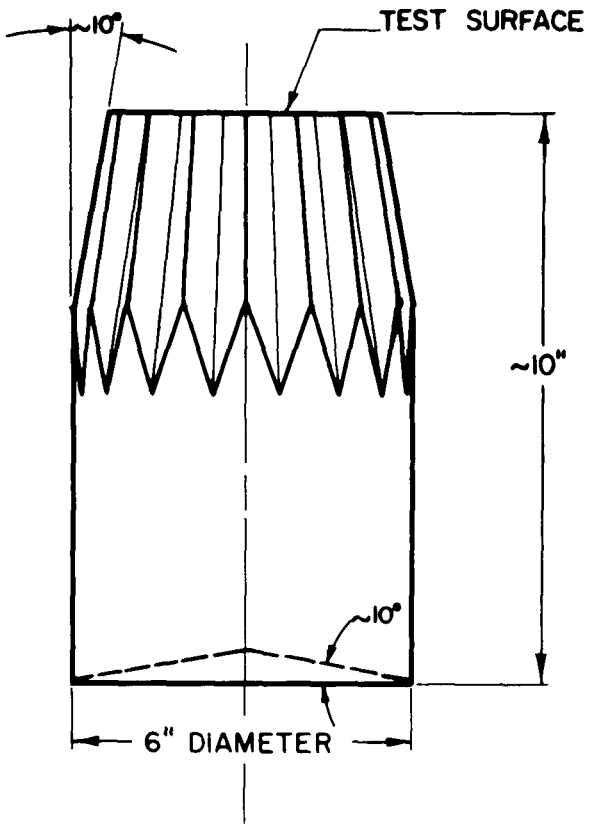

FIG. 1 SKETCH OF SPECIMEN

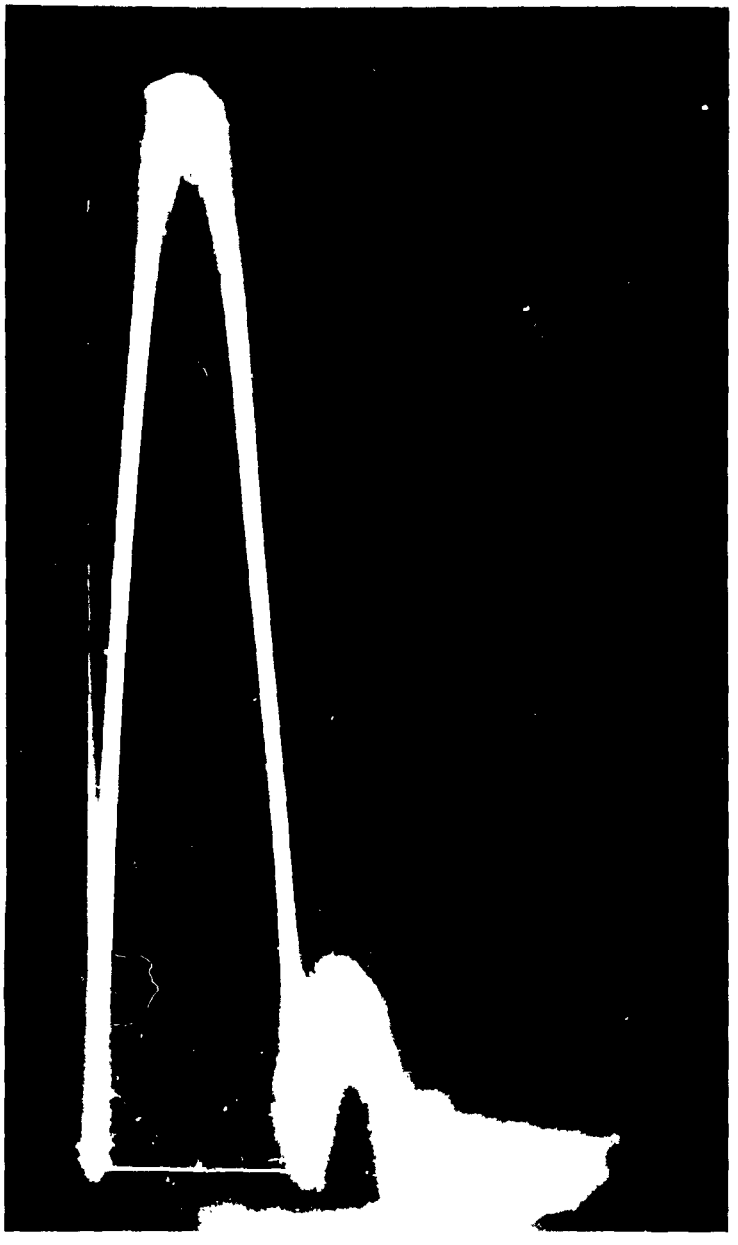

Figure 2. Ball in free fall bouncing from specimen surface. (Photograph is of 1" steel ball striking annealed specimen of 6061-T6 aluminum at 443 cm/sec. Height of rebound = 7.8 cm.)

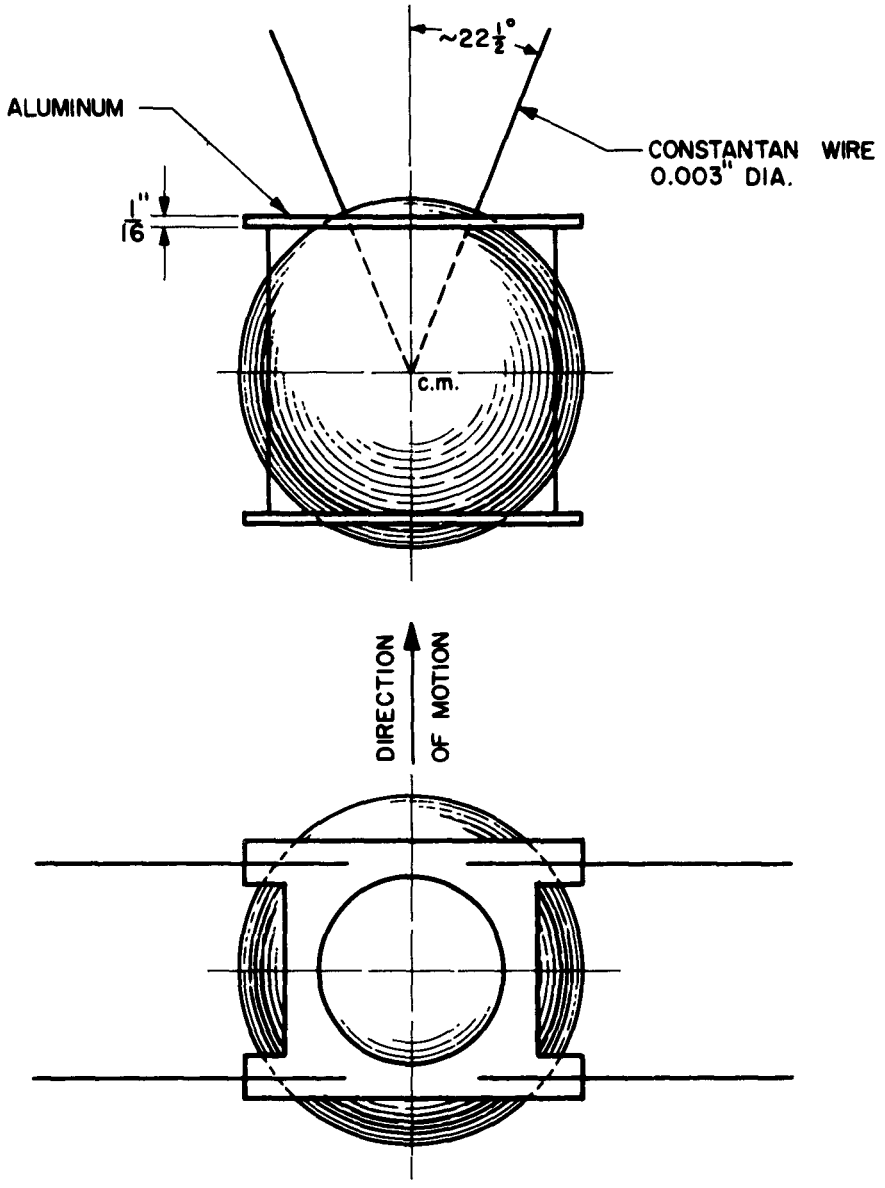

FIG. 3 SUSPENSION SYSTEM FOR INDENTING BALL

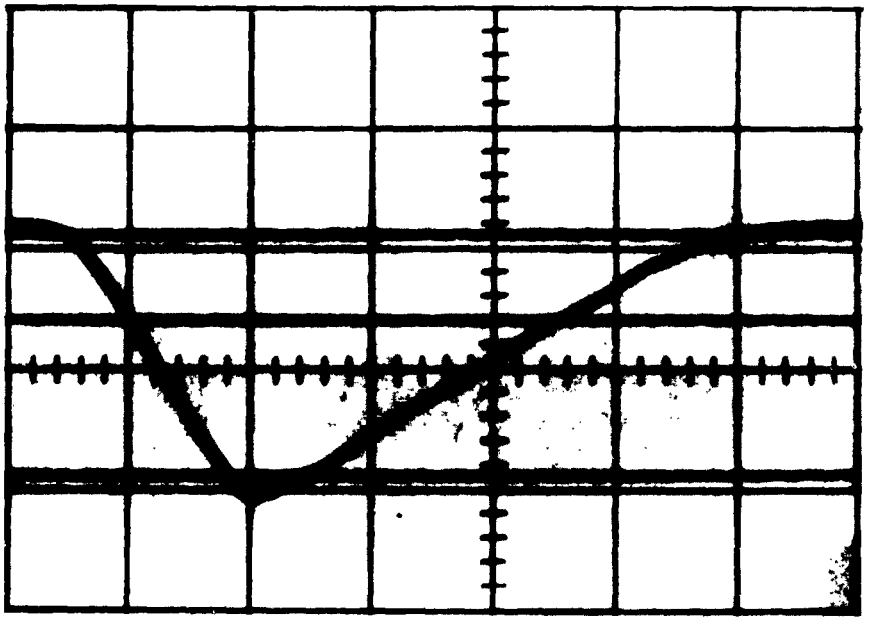

Figure 4. Oscilloscope pattern showing travel of ball suspended as a simple pendulum. (Time scale is horizontal: 20 divisions = 1 second. Ball approaches from the left. Distance from specimen is indicated by the two heavy horizontal lines: the top line is 10 mm. and the bottom 1 mm. away from the specimen.

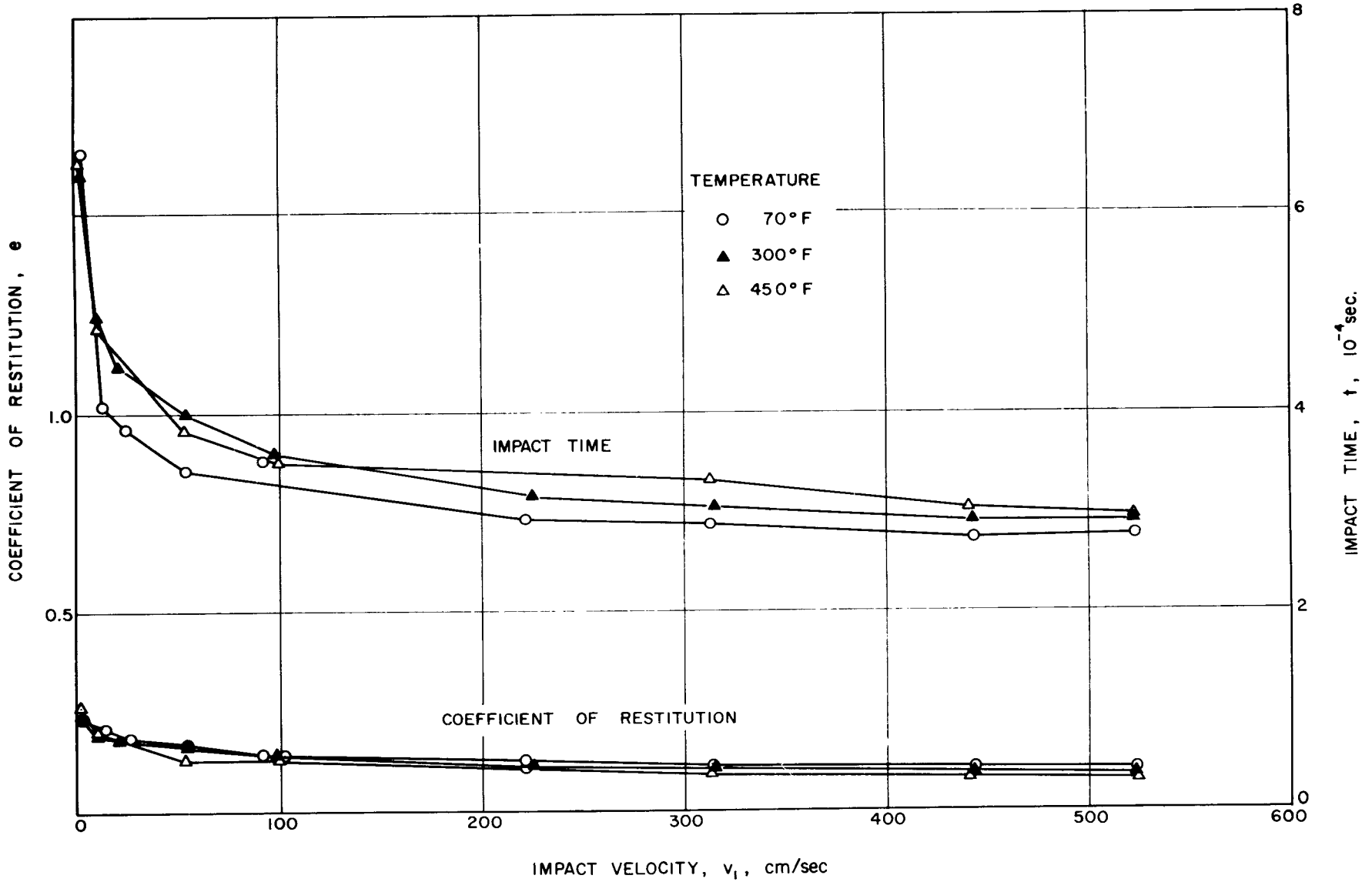

FIG. 5 COEEFICIENT OF RESTITUTION AND IMPACT TIME FOR 1" STEEL BALL STRIKING LEAD SPECIMEN

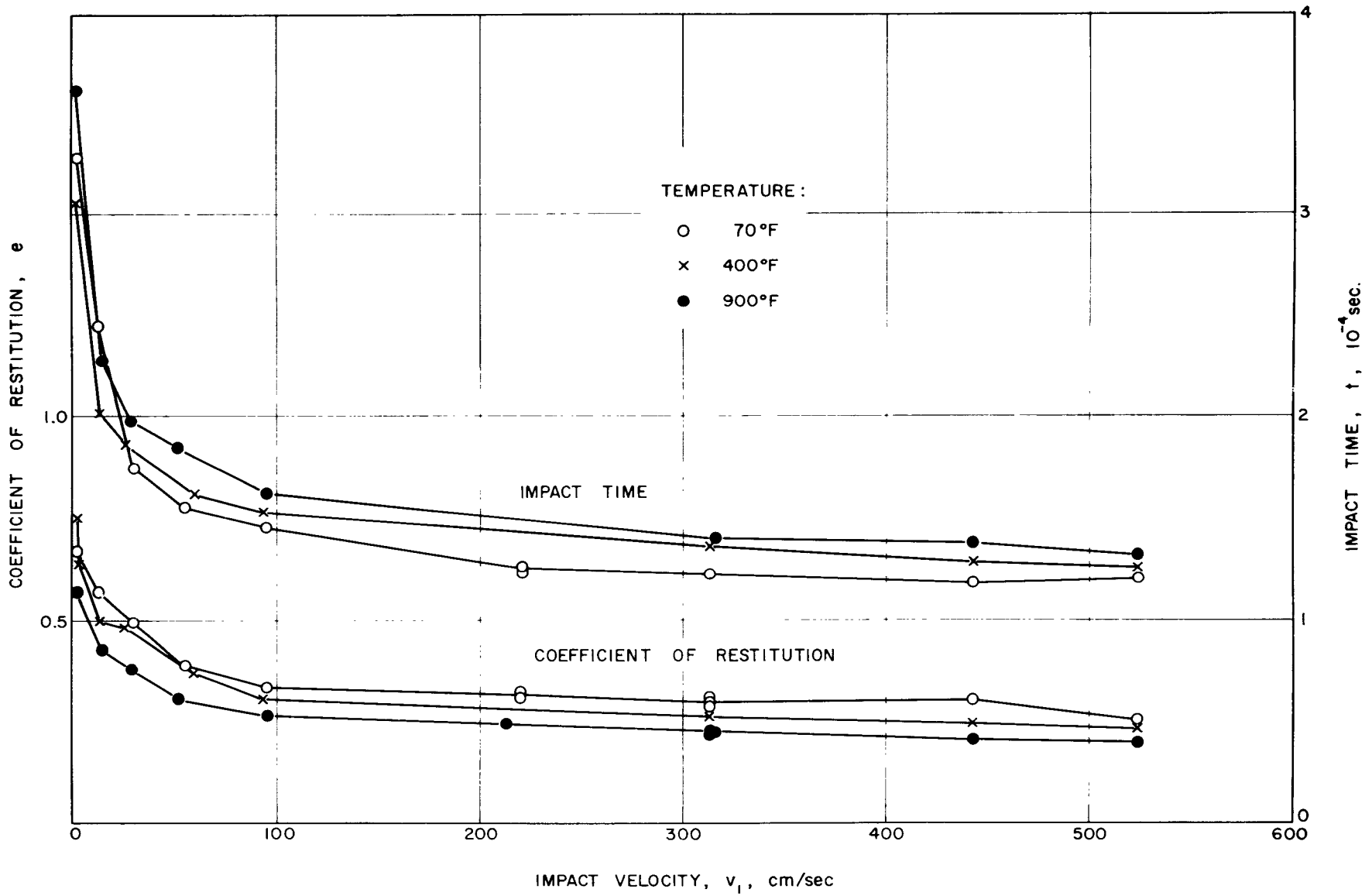

FIG. 6 COEFFICIENT OF RESTITUTION AND IMPACT TIME FOR 1" STEEL BALL STRIKING ANNEALED SPECIMEN OF 6061 - T6 ALUMINUM

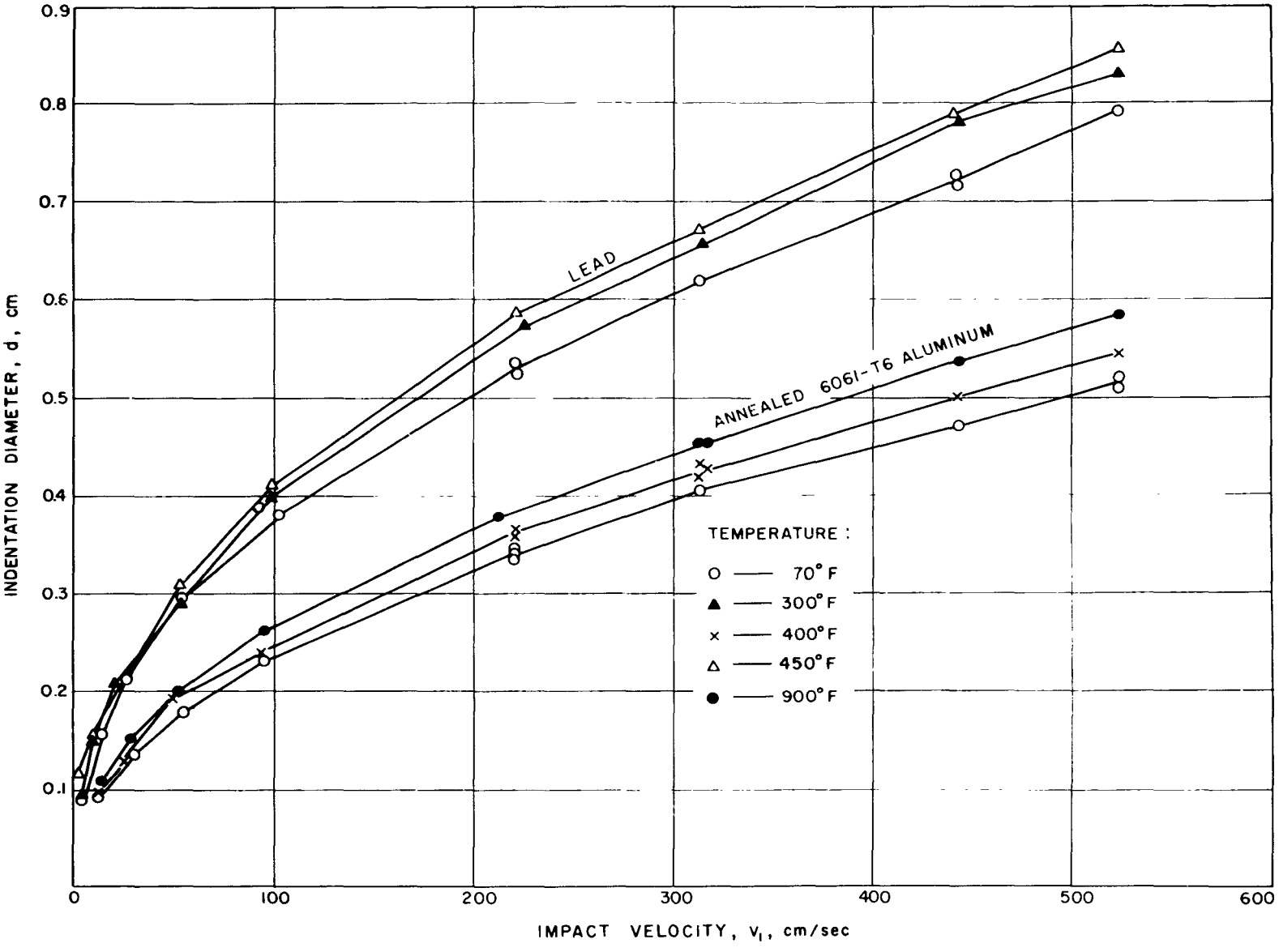

FIG.7 DIAMETER OF IDENTATION PRODUCED WITH 1" STEEL BALL

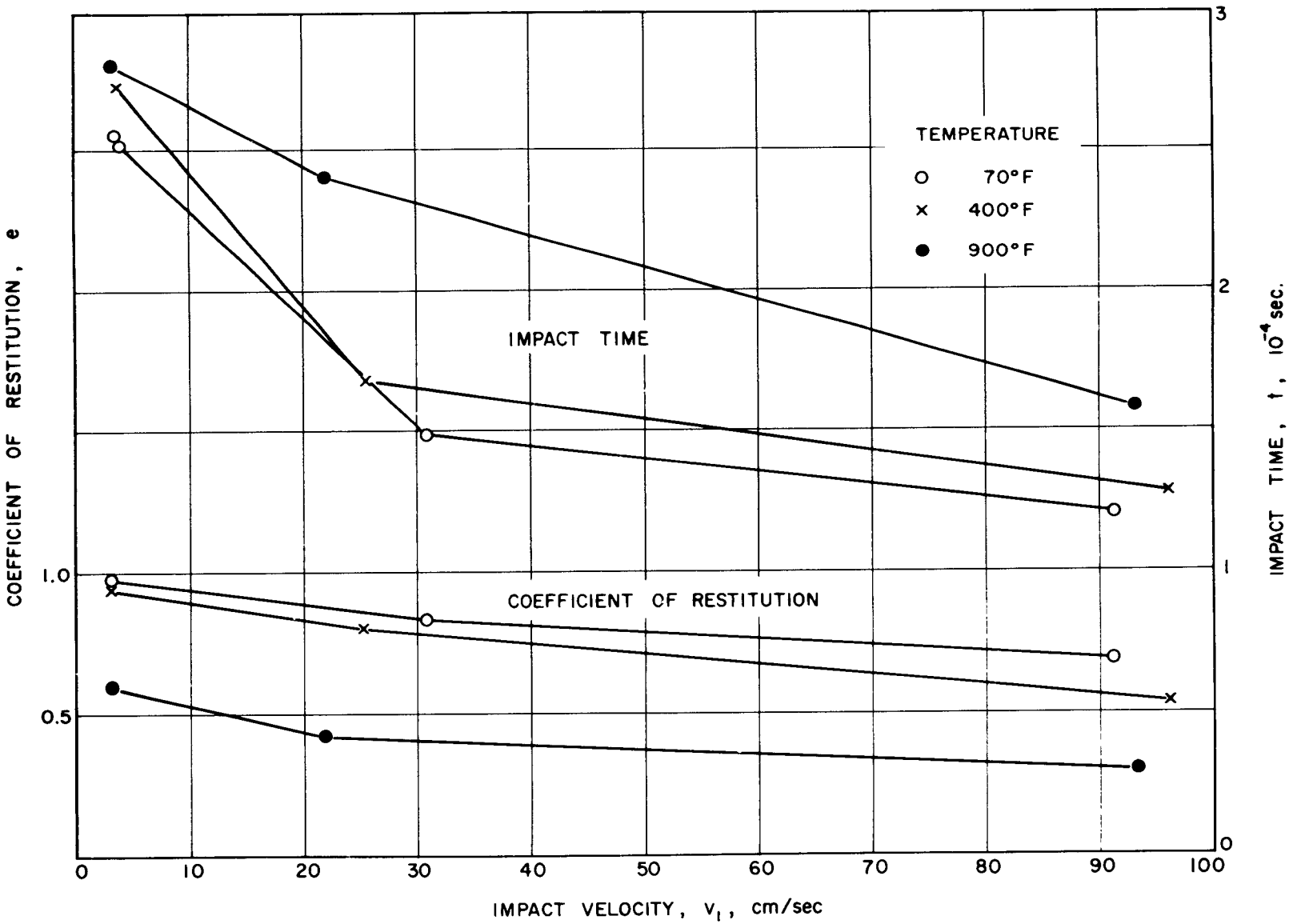

FIG. 8 COEFFICIENT OF RESTITUTION AND IMPACT TIME FOR 1" STEEL BALL STRIKING AS ROLLED SPECIMEN OF 6061 - T6 ALUMINUM

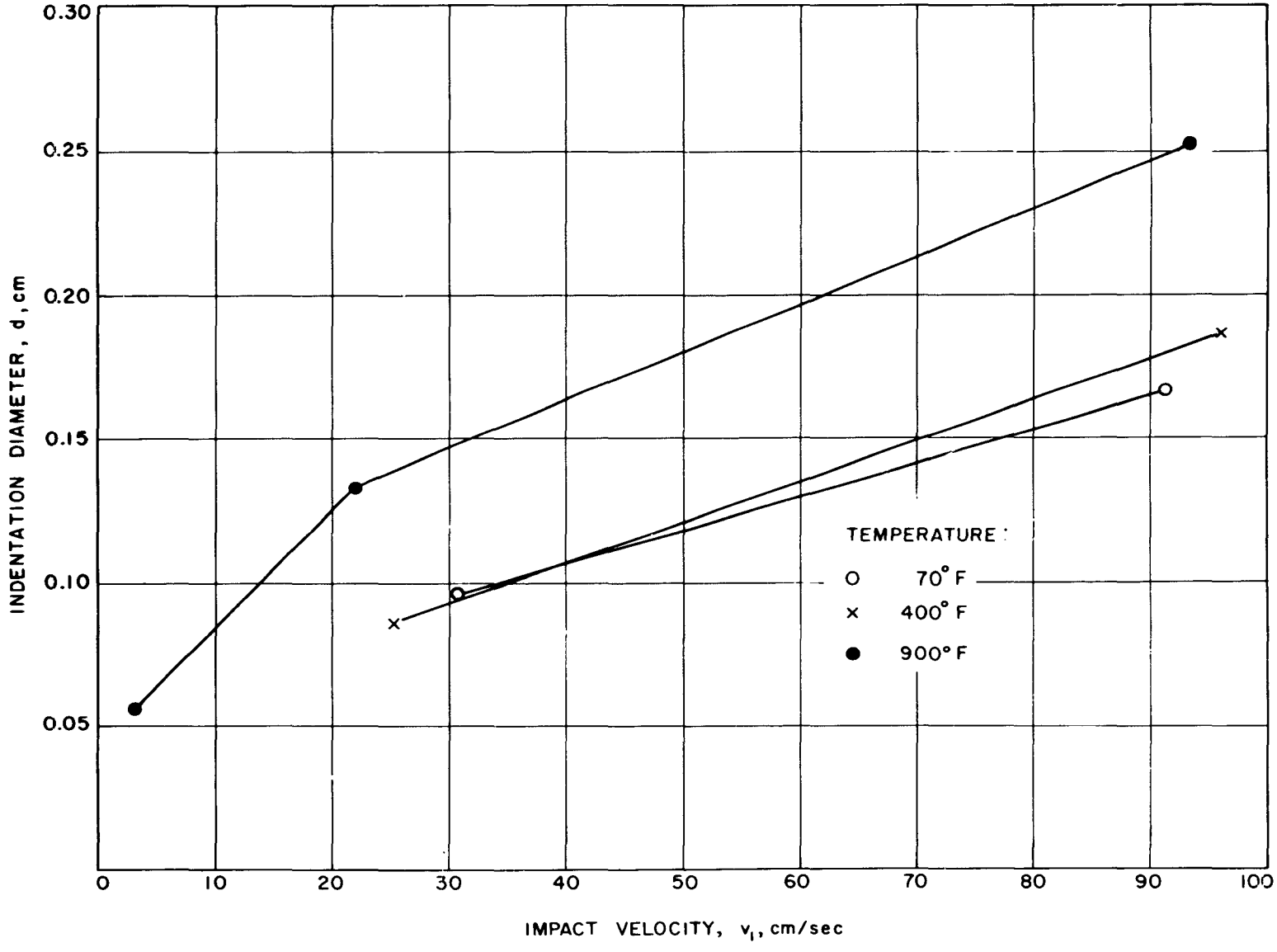

FIG. 9 INDENTATION DIAMETER FOR 1" STEEL BALL STRIKING AS ROLLED SPECIMEN OF 6061-T6 ALUMINUM

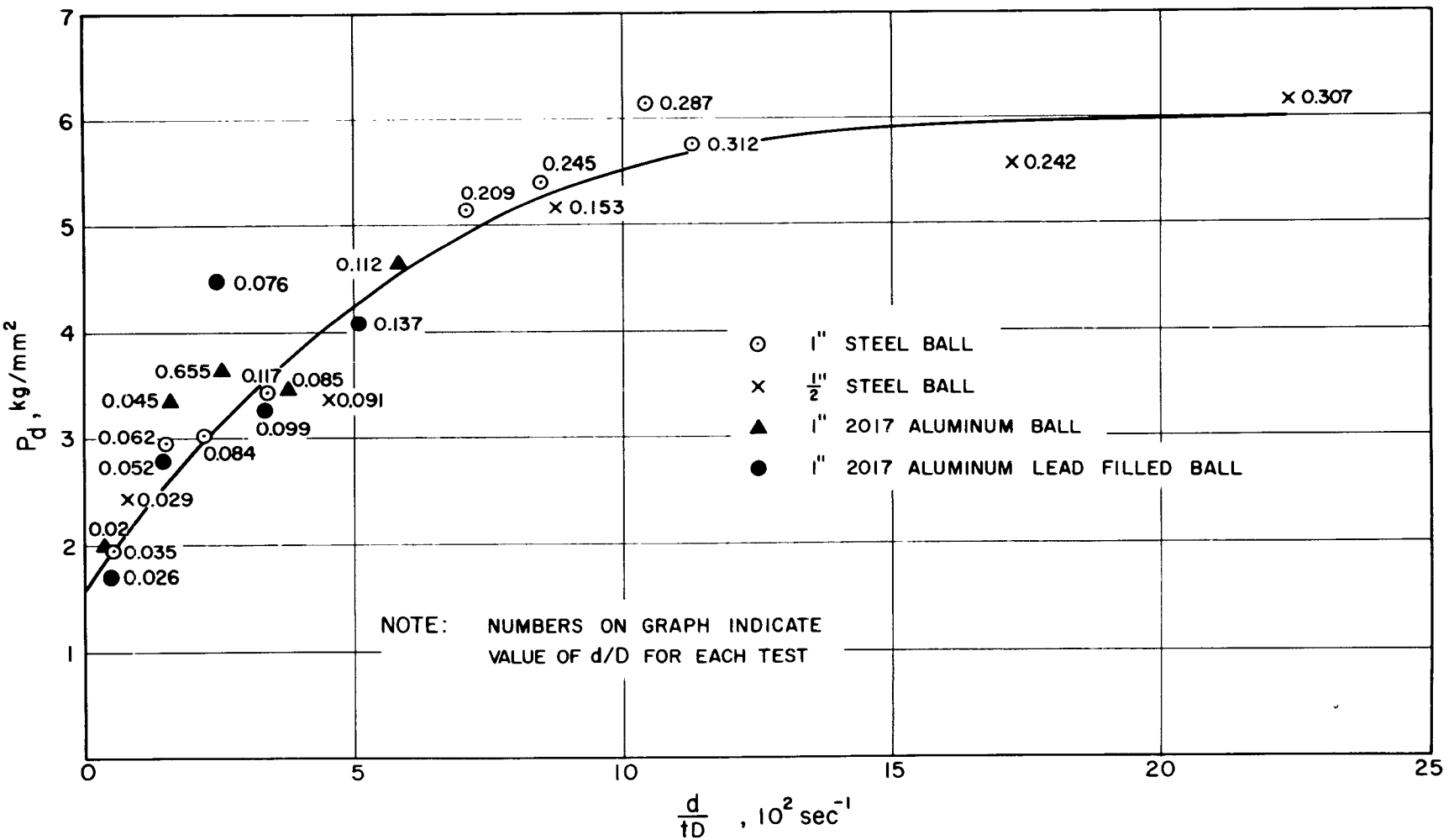

FIG. 10 DEPENDENCE OF P_d ON $\frac{d}{tD}$ FOR LEAD SPECIMEN AT ROOM TEMPERATURE

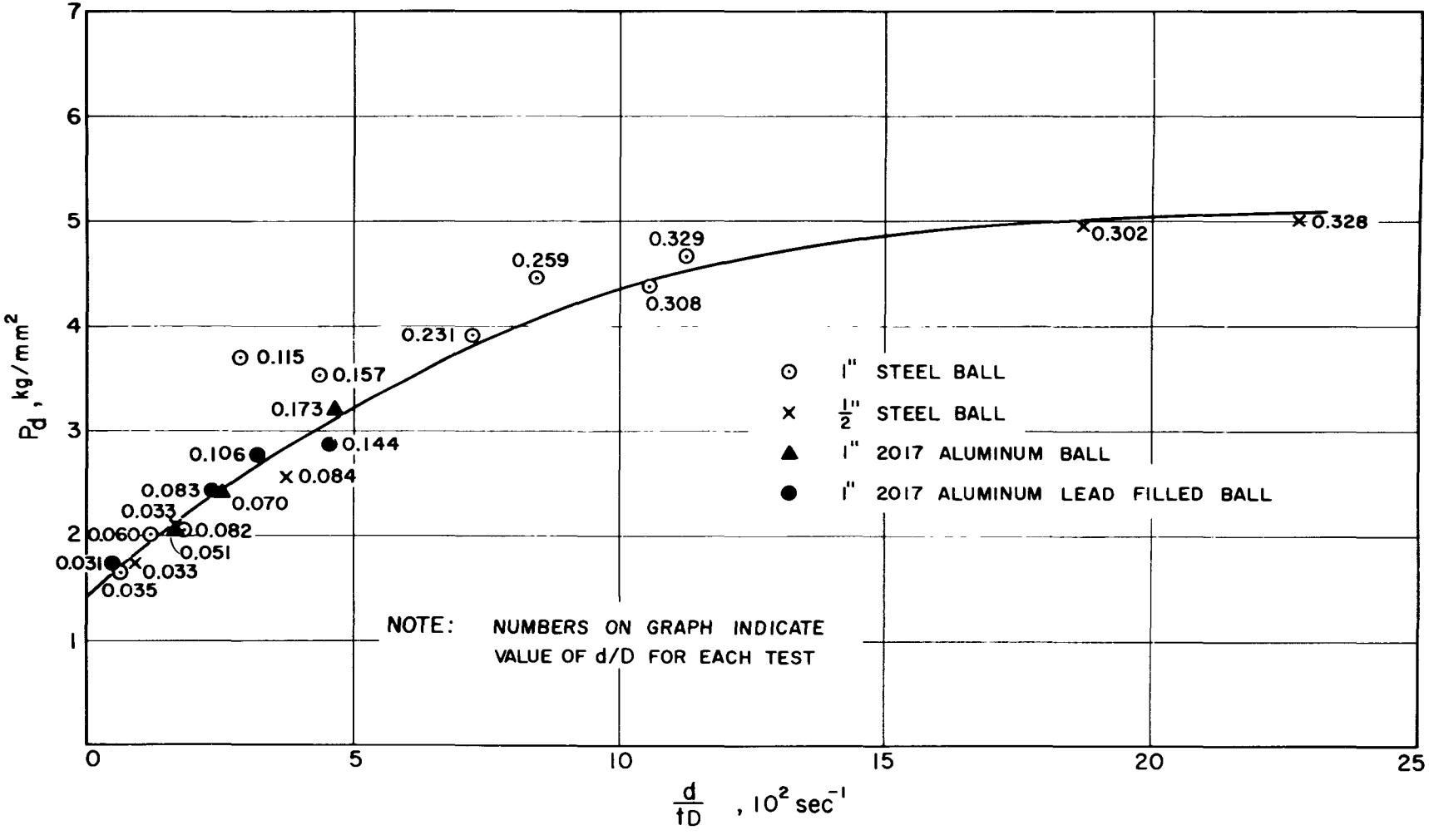

FIG. 11 DEPENDENCE OF P_d ON $\frac{d}{tD}$ FOR LEAD SPECIMEN AT 300°F

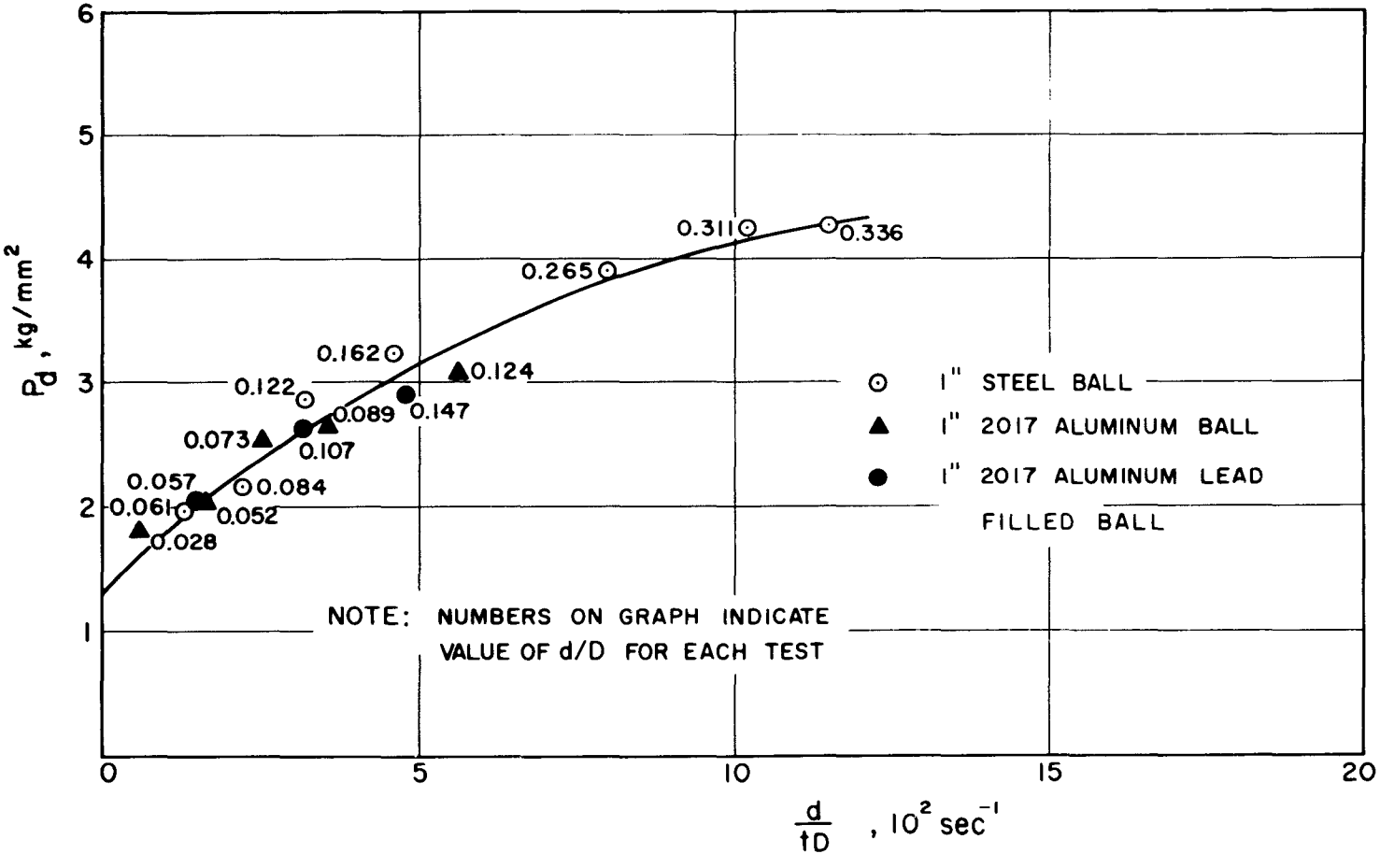

FIG. 12 DEPENDENCE OF P_d ON $\frac{d}{tD}$ FOR LEAD SPECIMEN AT 450°F

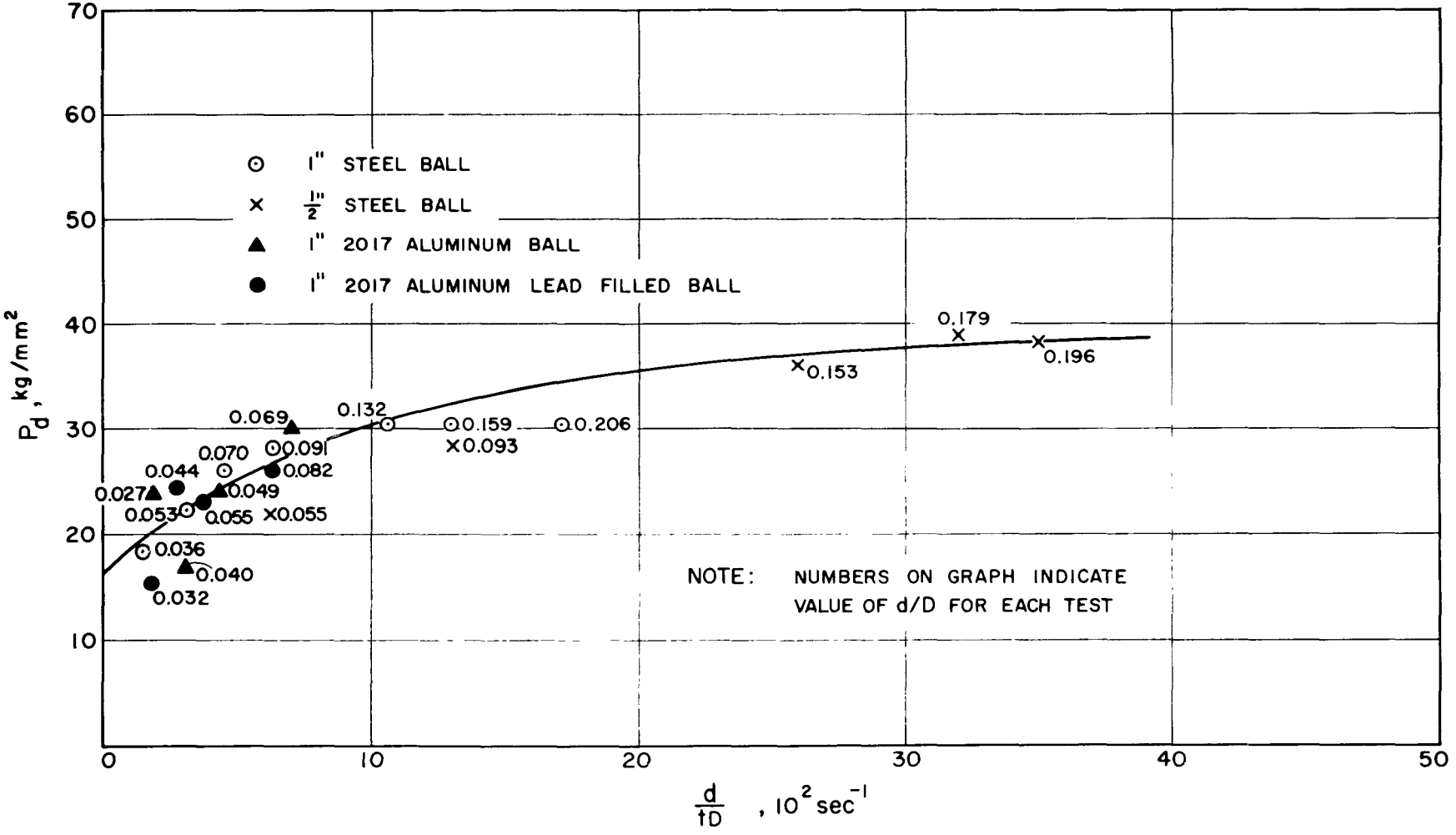

FIG. 13 DEPENDENCE OF P_d ON $\frac{d}{tD}$ FOR ANNEALED SPECIMEN OF 6061 - T6 ALUMINUM AT ROOM TEMPERATURE

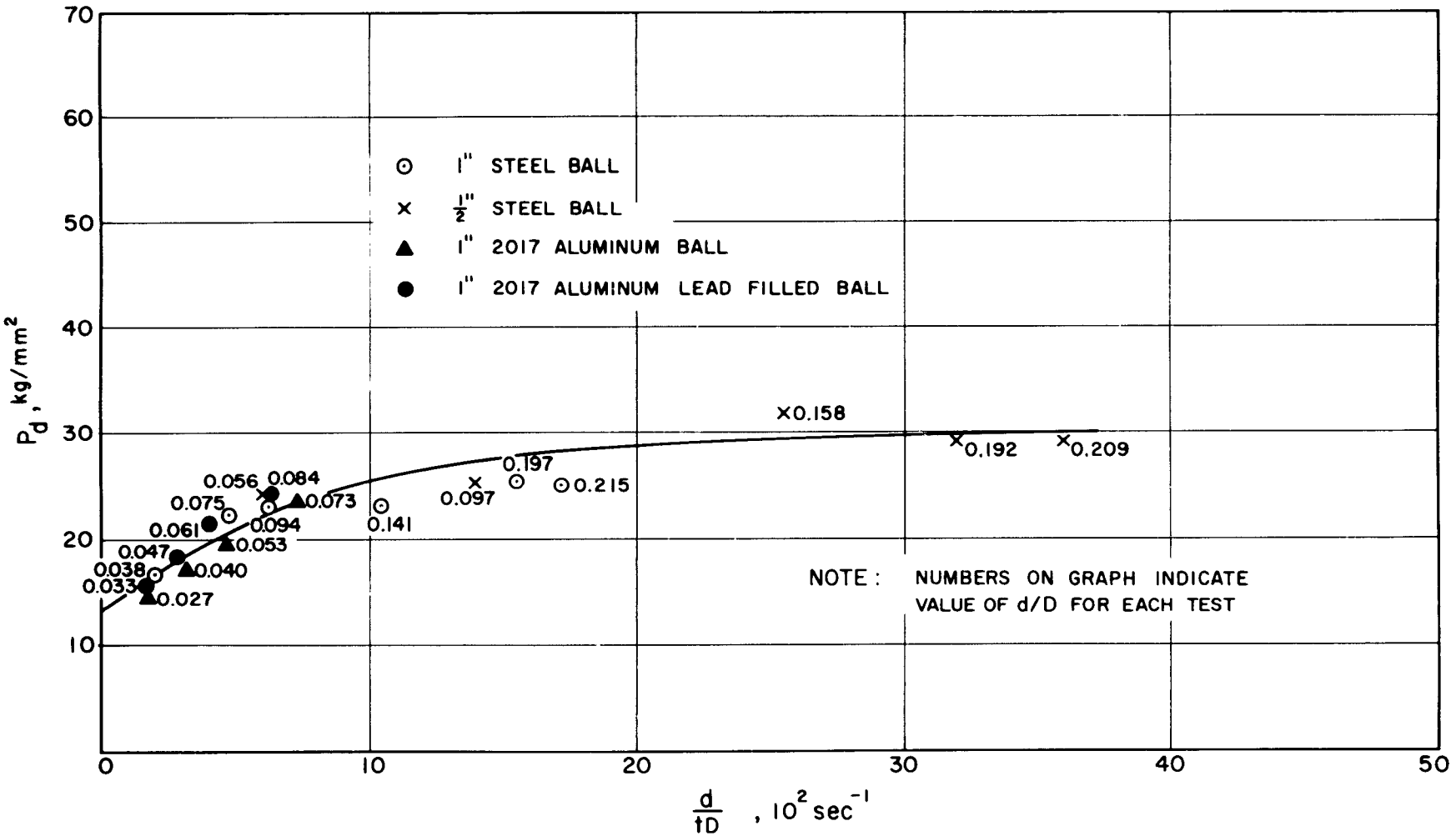

FIG. 14 DEPENDENCE OF P_d ON $\frac{d}{tD}$ FOR ANNEALED SPECIMEN OF 6061-T6 ALUMINUM AT 400°F

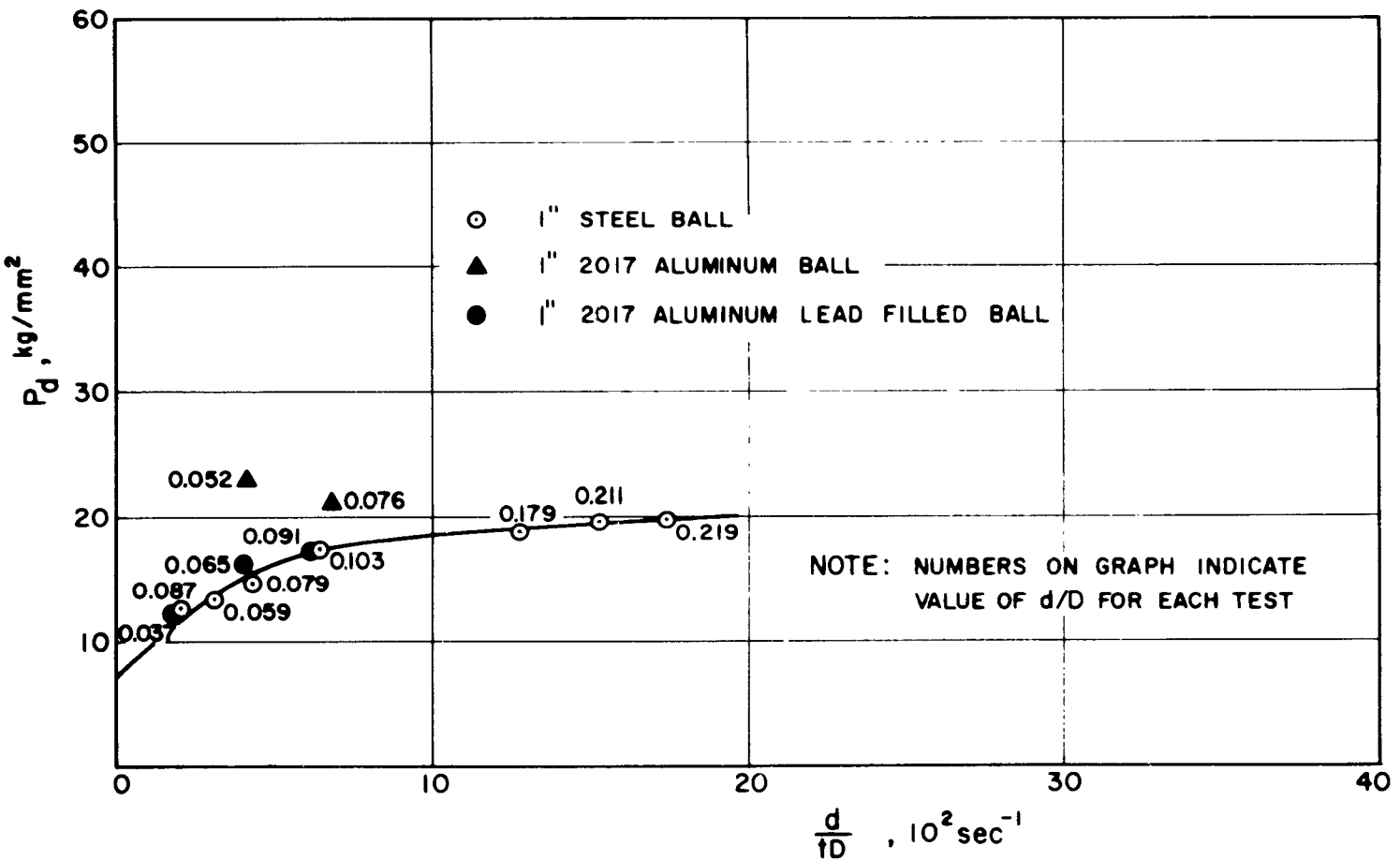

FIG. 15 DEPENDENCE OF P_d ON $\frac{d}{tD}$ FOR ANNEALED SPECIMEN OF 6061—T6 ALUMINUM AT 900°F

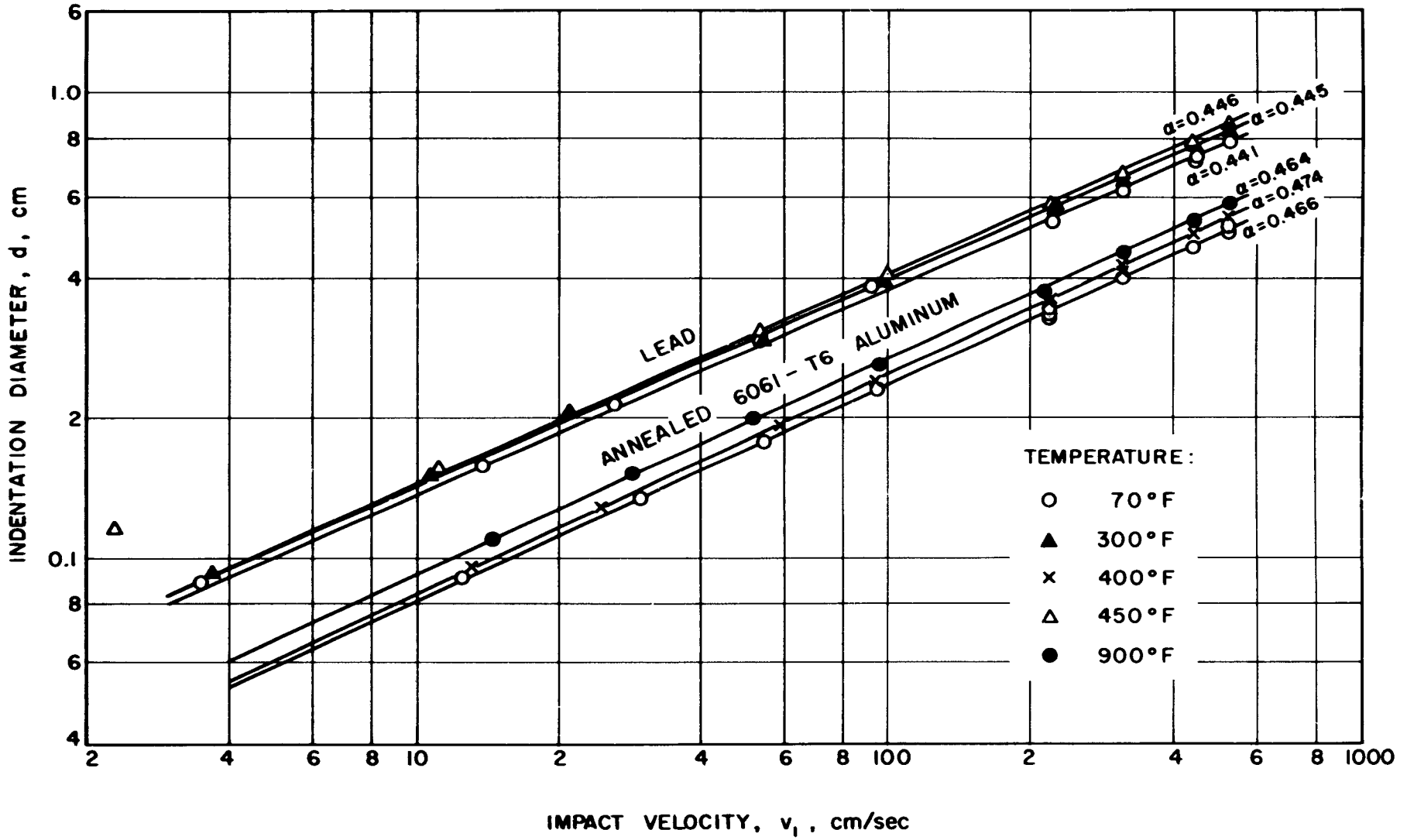

FIG. 16 RELATION BETWEEN LOG d AND LOG v_1 (INDENTER IS 1" STEEL BALL)

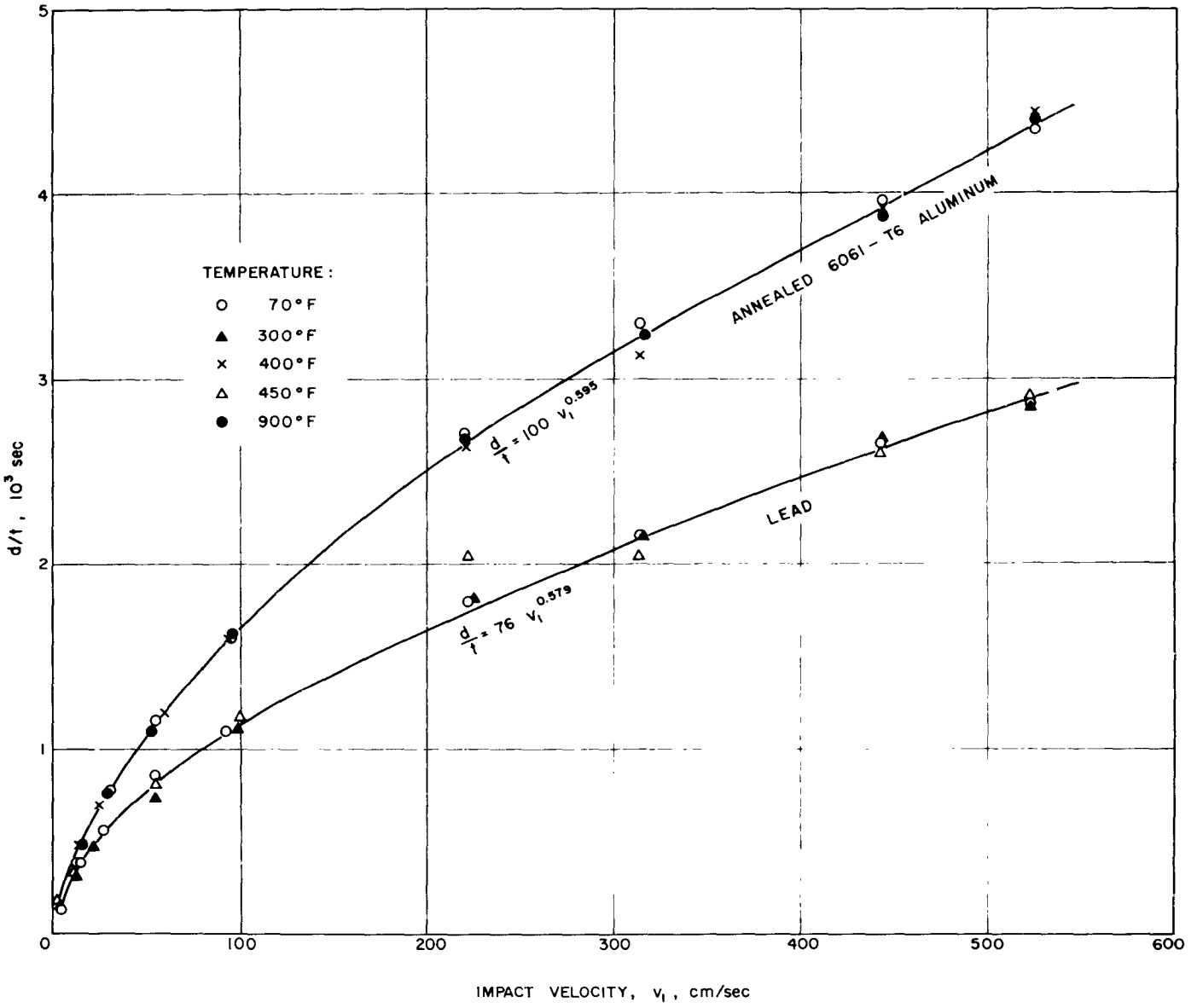

FIG. 17 DEPENDENCE OF d/t ON IMPACT VELOCITY, v_1 (INDENTER IS 1" STEEL BALL)

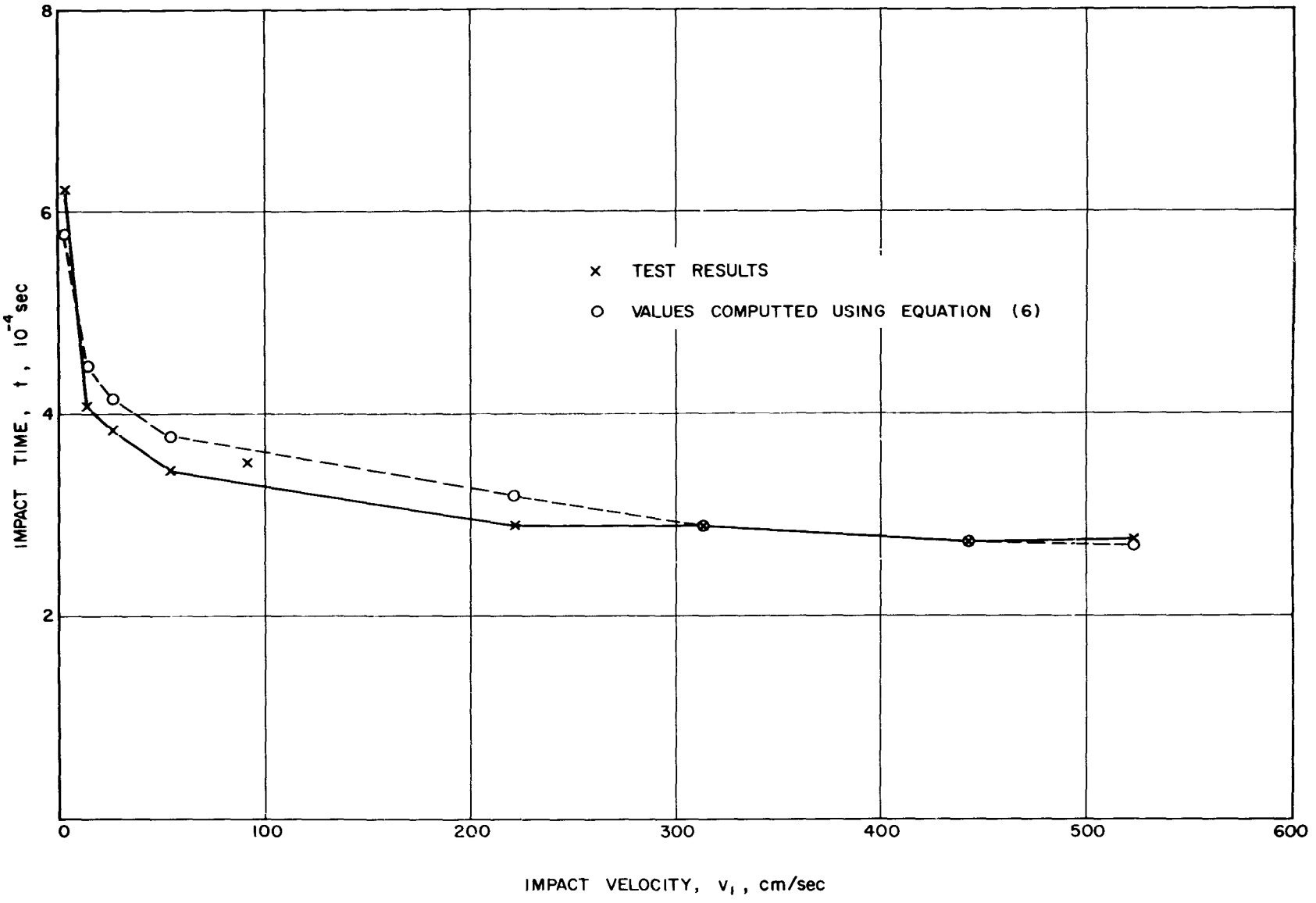

FIG. 18 TOTAL TIME OF IMPACT FOR 1" STEEL BALL STRIKING LEAD SPECIMEN AT ROOM TEMPERATURE

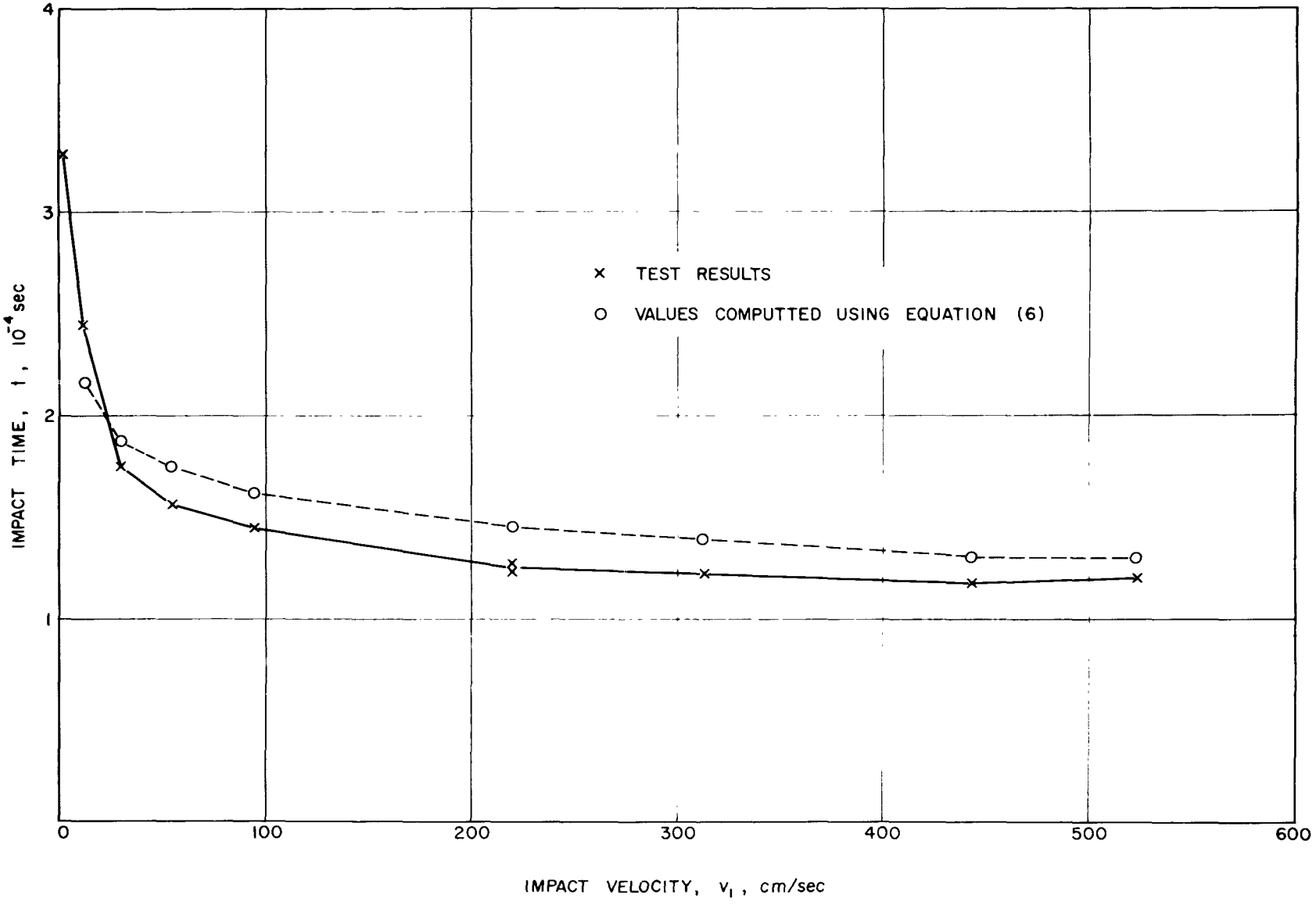

FIG. 19 TOTAL TIME OF IMPACT FOR 1" STEEL BALL STRIKING ANNEALED SPECIMEN OF 6061 - T6 ALUMINUM AT ROOM TEMPERATURE

DISTRIBUTION LIST FOR UNCLASSIFIED
TECHNICAL REPORTS ISSUED UNDER
Contract Nonr-562(20), Task Nr 064-424

Chief of Naval Research
Department of the Navy
Washington 25, D.C.
Attn: Code 438 (2)
Code 463 (1)

Commanding Officer
Officer of Naval Research
Branch Office
495 Summer Street
Boston 10, Massachusetts (1)

Commanding Officer
Office of Naval Research
Branch Office
John Crerar Library Building
86 E. Randolph Street
Chicago 11, Illinois (1)

Commandin Officer
Office of Naval Research
Branch Office
346 Broadway
New York 13, New York (1)

Commanding Officer
Office of Naval Research
Branch Office
1030 E. Green Street
Pasadena, California (1)

Commanding Officer
Office of Naval Research
Branch Office
1000 Geary Street
San Francisco, California (1)

Commanding Officer
Office of Naval Research
Navy #100, Fleet Post Office
New York, New York (25)

Director
Naval Research Laboratory
Washington 25, D.C.
Attn: Tech. Info. Officer (6)
Code 6200 (1)
Code 6205 (1)
Code 6250 (1)
Code 6260 (1)

Armed Services Technical
Information Agency
ATTN: TIPCR
Arlington Hall Station
Arlington 12, Virginia (10)

Office of Technical Services
Department of Commerce
Washington 25, D.C. (1)

Office of the Secretary of
Defense
Research and Development Division
The Pentagon
Washington 25, D.C.
Attn: Technical Library (1)

Chief
Armed Forces Special Weapons
Project
The Pentagon
Washington 25, D.C.
Attn: Technical Information
Division (2)
Weapons Effects Div. (1)
Special Field Projects(1)
Blast and Shock Branch(1)

Office of the Secretary of
the Army
The Pentagon
Washington 25, D.C.
Attn: Army Library (1)

Chief of Staff
Department of the Army
Washington 25, D.C.
Attn: Development Branch
Res. and Dev. Division(1)
Research Branch
Res. and Dev. Division(1)
Special Weapons Branch
Res. and Dev. Division(1)

Commanding Officer
Engineer Research Development
Laboratory
Fort Belvoir, Virginia (1)

Office of the Chief of Ordnance
Department of the Army
Washington 25, D.C.
Attn: Research and Materials Branch
(Ord. Res. and Dev. Div.) (1)

Office of the Chief of Engineers
Department of the Army
Washington 25, D.C.
Attn: ENG-HL Lib. Br., Adm. Ser. Div. (1)
ENG-WE Eng. Div., Civil Works (1)
ENG-EB Prot. Constr. Br., Eng. Div., Mil. Constr. (1)
ENG-WD Planning Div. Civil Works (1)
ENG-EA Struc. Br., Eng. Div., Mil. Constr. (1)
ENG-NB Special Engr. Br., Eng. Res. and Dev. Division (1)

Office of the Chief Signal Officer
Department of the Army
Washington 25, D.C.
Attn: Engineering and Technical Division (1)

Commanding Officer
Watertown Arsenal
Watertown, Massachusetts
Attn: Laboratory Division (1)

Commanding Officer
Frankford Arsenal
Bridesburg Station
Philadelphia 37, Pennsylvania
Attn: Laboratory Division (1)

Office of Ordnance Research
2127 Myrtle Drive
Duke Station
Durham, North Carolina
Attn: Division of Engineering Sciences (1)

Commanding Officer
Squier Signal Laboratory
Fort Monmouth, New Jersey
Attn: Components and Materials Branch (1)

Chief of Naval Operations
Department of the Navy
Washington 25, D.C.
Attn: Op 37 (1)

Commandant, Marine Corps
Headquarters, U.S. Marine Corps.
Washington 25, D.C. (1)

Chief, Bureau of Ships
Department of the Navy
Washington 25, D.C.
Attn: Code 312 (2)
(1)
(1)
Code 420 (1)
Code 423 (2)
Code 442 (2)

Chief, Bureau of Aeronautics
Department of the Navy
Washington 25, D.C.
Attn: AE-4 (1)
AV-34 (1)
AD (1)
AD-2 (1)
TD-42 (1)
RS-7 (1)
RS-8 (1)

Chief, Bureau of Ordnance
Department of the Navy
Washington 25, D.C.
Attn: Ad3 (1)
Re (1)
Res (1)
Reu (1)
ReS5 (1)
ReS1 (1)
Ren (1)

Chief, Bureau of Yards and Docks
Department of the Navy
Washington 25, D.C.
Attn: Code D-202 (1)
Code D-202.3 (1)
Code D-220 (1)
Code D-222 (1)
Code D-410C (1)
Code D-440 (1)
Code D-500 (1)

Commanding Officer and Director
David Taylor Model Basin
Washington 7, D.C.
Attn: Code 140 (1)
Code 600 (1)
Code 700 (1)
Code 720 (1)
Code 725 (1)
Code 731 (1)
Code 740 (1)

U. S. Naval Ordnance Laboratory
White Oak, Maryland
Attn: Technical Library (2)
Technical Evaluation Department (1)

Director
Materials Laboratory
New York Naval Shipyard
Brooklyn 1, New York (1)

Commanding Officer and Director
U. S. Naval Electronics Laboratory
San Diego 52, California (1)

Officer-in-Charge
Naval Civil Engineering Research and Evaluation Laboratory
U. S. Naval Construction Battalion Center
Port Hueneme, California (2)

Director
Naval Air Experimental Station
Naval Air Material Center
Naval Base
Philadelphia 12, Pennsylvania
Attn: Materials Laboratory (1)
Structures Laboratory (1)

Officer-in-Charge
Underwater Explosion Research Division
Norfolk Naval Shipyard
Portsmouth, Virginia
Attn: Dr. A. H. Keil (2)

Commander
U. S. Naval Proving Grounds
Dahlgren, Virginia (1)

Commander
Naval Ordnance Test Station
Inyokern, China Lake, California
Attn: Physics Division (1)
Mechanics Branch (1)

Commanding Officer and Director
Naval Engineering Experimental Station
Annapolis, Maryland (1)

Commanding Officer
USNNOEU
Kirtland Air Force Base
Albuquerque, New Mexico
Attn: Code 20
(Dr. J. N. Brennen) (1)

Superintendent
Naval Post Graduate School
Monterey, California (1)

Commandant
Marine Corps School
Quantico, Virginia
Attn: Director, Marine Corps Development Center (1)

Commanding General
U. S. Air Force
Washington 25, D.C.
Attn: Research and Development Division (1)

Commander
Air Material Command
Wright-Patterson Air Force Base
Dayton, Ohio
Attn: MCREX-B (1)
Structures Division (1)

Commander
U. S. Air Force Institute of Technology
Wright-Patterson Air Force Base
Dayton, Ohio
Attn: Chief, Applied Mechanics Group (1)

Director of Intelligence
Headquarters, U. S. Air Force
Washington 25, D.C.
Attn: P. V. Branch
(Air Targets Division) (1)

Commander
Air Force Office of Scientific Research
Washington 25, D.C.
Attn: Mechanics Division (1)

U. S. Atomic Energy Commission
Washington 25, D.C.
Attn: Director of Research (2)

Director
National Bureau of Standards
Washington 25, D.C.
Attn: Division of Mechanics (1)
Engineering Mechanics Section (1)
Aircraft Structures (1)

Commandant
U.S. Coast Guard
1300 E. Street, N. W.
Washington 25, D.C.
Attn: Chief, Testing and Development Division (1)

U. S. Maritime Administration
General Administration Office Building
Washington 25, D.C.
Attn: Chief, Division of Preliminary Design (1)

National Aeronautics and Space Administration
1515 H Street, N. W.
Washington 25, D.C.
Attn: Loads and Structures Division (2)

Director
Langley Aeronautical Laboratory
Langley Field, Virginia
Attn: Structures Division (2)

Director
Forest Products Laboratory
Madison, Wisconsin (1)

Civil Aeronautics Administration
Department of Commerce
Washington 25, D.C.
Attn: Chief, Aircraft Engineering Division (1)
Chief, Airframe and Equipment Branch (1)

National Sciences Foundation
1951 Constitution Avenue, N.W.
Washington, D.C.
Attn: Engineering Sciences Division (1)

National Academy of Sciences
2101 Constitution Avenue
Washington 25, D.C.
Attn: Technical Director, Committee on Ships Structural Design (1)
Executive Secretary, Committee on Undersea Warfare (1)

Professor Lynn S. Beedle
Fritz Engineering Laboratory
Lehigh University
Bethlehem, Pennsylvania (1)

Professor R. L. Bisplinghoff
Dept. of Aeronautical Engineering
Massachusetts Institute of Technology
Cambridge 39, Massachusetts (1)

Professor H. H. Bleich
Department of Civil Engineering
Columbia University
New York 27, New York (1)

Professor B. A. Boley
Department of Civil Engineering
Columbia University
New York 27, New York (1)

Professor G. F. Carrier
Pierce Hall
Harvard University
Cambridge 38, Massachusetts (1)

Professor Herbert Deresiewicz
Dept. of Mechanical Engineering
Columbia University
632 W. 125th Street
New York 27, New York (1)

Professor D. C. Drucker
Division of Engineering
Brown University
Providence 12, Rhode Island (1)

Professor A. C. Eringen
Division of Engineering Sciences
Purdue University
Lafayette, Indiana (1)

Professor W. Flügge
Dept. of Aeronautical Engineering
Stanford University
Stanford, California (1)

Professor J. N. Goodier
Dept. of Engineering Mechanics
Stanford University
Stanford, California (1)

Professor L. E. Goodman
Engineering Experiment Station
University of Minnesota
Minneapolis, Minnesota (1)

Professor M. Hetenyi
The Technological Institute
Northwestern University
Evanston, Illinois (1)

Professor P. G. Hodge
Department of Mechanics
Illinois Institute of Technology
Chicago 16, Illinois (1)

Professor N. J. Hoff
Dept. of Aeronautical Engineering
Stanford University
Stanford, California (1)

Professor W. H. Hoppmann, II
Department of Mechanics
Rensselaer Polytechnic Institute
Troy, New York (1)

Professor Bruce G. Johnston
University of Michigan
Ann Arbor, Michigan (1)

Professor J. Kempner
Dept. of Aeronautical Engineering
and Applied Mechanics
Polytechnic Institute of Brooklyn
99 Livingston Street
Brooklyn 2, New York (1)

Professor H. L. Langhaar
Dept. of Theoretical and
Applied Mechanics
University of Illinois
Urbana, Illinois (1)

Professor B. J. Lazan, Director
Engineering Experiment Station
University of Minnesota
Minneapolis 14, Minnesota (1)

Professor E. H. Lee
Division of Applied Mathematics
Brown University
Providence 12, Rhode Island (1)

Professor Paul Lieber
Geology Department
University of California
Berkeley 4, California (1)

Professor Hsu Lo
School of Engineering
Purdue University
Lafayette, Indiana (1)

Professor R. D. Mindlin
Department of Civil Engineering
Columbia University
632 W. 125th Street
New York 27, New York (1)

Dr. A. Nadai
136 Cherry Valley Road
Pittsburgh 21, Pennsylvania (1)

Professor Paul M. Naghdi
Mech. Engin., Mechanics & Design
University of California
Berkeley 4, California (1)

Professor William A. Nash
Dept.of Engineering Mechanics
University of Florida
Gainesville, Florida (1)

Professor N. M. Newmark, Head
Department of Civil Engineering
University of Illinois
Urbana, Illinois (1)

Professor Aris Phillips
Department of Civil Engineering
15 Prospect Street
Yale University
New Haven, Connecticut (1)

Professor W. Prager
Computing Center
Brown University
Providence 12, Rhode Island (1)

Professor E. Reissner
Department of Mathematics
Massachusetts Institute of
Technology
Cambridge 39, Massachusetts (1)

Professor M. A. Sadowsky
Department of Mechanics
Rensselaer Polytechnic Institute
Troy, New York (1)

Professor J. Stallmeyer
Department of Civil Engineering
University of Illinois
Urbana, Illinois (1)

Professor Eli Sternberg
Division of Applied Mathematics
Brown University
Providence 12, Rhode Island (1)

Professor S. P. Timoshenko
School of Engineering
Stanford University
Stanford, California (1)

Professor A. S. Velestos
Department of Civil Engineering
University of Illinois
Urbana, Illinois (1)

Professor Enrico Volterra
Dept. of Engineering Mechanics
University of Texas
Austin, Texas (1)

Dr. Dana Young
Southwest Research Institute
8500 Culebra Road
San Antonio 6, Texas (1)

Professor Bernard W. Shaffer
Dept. of Mechanical Engineering
New York University
New York 53, New York (1)

Dr. John F. Brahtz
Southern California Laboratories
Stanford Research Institute
820 Mission Street (1)
South Pasadena, California

Mr. Martin Goland, President
Southwest Research Institute
8500 Culebra Road
San Antonio, Texas (1)

Mr. S. Levy
Midwest Research Institute
Kansas City, Missouri

(1)

Nonr-562(20) Distribution List (7)

Professor B. Budiansky
Dept. of Mechanical Engineering
School of Applied Sciences
Harvard University
Cambridge 38, Massachusetts (1)

Professor George Herrmann
Department of Civil Engineering
Columbia University
New York 27, New York (1)

Professor E. Orowan
Dept. of Mechanical Engineering
Massachusetts Institute of Technology
Cambridge 39, Massachusetts (1)

Professor J. Ericksen
Mechanical Engineering Department
Johns Hopkins University
Baltimore 18, Maryland (1)

Professor T. Y. Thomas
Graduate Institute for Mathematics and Mechanics
Indiana University
Bloomington, Indiana (1)

Professor Joseph Marin, Head
Department of Engineering Mechanics
College of Engineering and Architecture
The Pennsylvania State University
University Park, Pennsylvania (1)

Professor Robert L. Ketter
Department of Civil Engineering
University of Buffalo
Buffalo 14, New York (1)

Mr. K. H. Koopman, Secretary
Welding Research Council of The Engineering Foundation
29 W 39th Street
New York 18, New York (2)

Professor Walter T. Daniels
School of Engineering and Architecture
Howard University
Washington 1, D.C. (1)

Professor P. S. Symonds, Chairman
Division of Engineering
Brown University
Providence 12, Rhode Island (1)

Professor Nicholas Perrone
Engineering Science Department
Pratt Institute
Brooklyn 5, New York (1)

Commander
Wright Air Development Center
Wright-Patterson Air Force Base
Dayton, Ohio
Attn: Dynamics Branch (1)
Aircraft Laboratory (1)
WCLSY (1)

Dr. Edward Wenk, Jr.
Executive Secretary
Federal Council for Science & Technology
The White House
Washington, D. C. (1)

Dr. H. G. Hopkins
War Office
Armament Research and Development Establishment
Fort Halstead
Sevenoaks, Kent, England (1)

Professor J. E. Cermak
Department of Civil Engineering
Colorado State University
Fort Collins, Colorado (1)

Professor W. J. Hall
Department of Civil Engineering
University of Illinois
Urbana, Illinois (1)

Professor R. Muki
Division of Mechanical Engineering
Keio University
Koganei-shi
Tokyo, Japan (1)

Nonr-562(20) Distribution List

(7)

Professor B. Budiansky
Dept. of Mechanical Engineering
School of Applied Sciences
Harvard University
Cambridge 38, Massachusetts (1)

Professor George Herrmann
Department of Civil Engineering
Columbia University
New York 27, New York (1)

Professor E. Orowan
Dept. of Mechanical Engineering
Massachusetts Institute of Technology
Cambridge 39, Massachusetts (1)

Professor J. Ericksen
Mechanical Engineering Department
Johns Hopkins University
Baltimore 18, Maryland (1)

Professor T. Y. Thomas
Graduate Institute for Mathematics and Mechanics
Indiana University
Bloomington, Indiana (1)

Professor Joseph Marin, Head
Department of Engineering Mechanics
College of Engineering and Architecture
The Pennsylvania State University
University Park, Pennsylvania (1)

Professor Robert L. Ketter
Department of Civil Engineering
University of Buffalo
Buffalo 14, New York (1)

Mr. K. H. Koopman, Secretary
Welding Research Council of The Engineering Foundation
29 W 39th Street
New York 18, New York (2)

Professor Walter T. Daniels
School of Engineering and Architecture
Howard University
Washington 1, D.C. (1)

Professor P. S. Symonds, Chairman
Division of Engineering
Brown University
Providence 12, Rhode Island (1)

Professor Nicholas Perrone
Engineering Science Department
Pratt Institute
Brooklyn 5, New York (1)

Commander
Wright Air Development Center
Wright-Patterson Air Force Base
Dayton, Ohio
Attn: Dynamics Branch (1)
Aircraft Laboratory (1)
WCLSY (1)

Dr. Edward Wenk, Jr.
Executive Secretary
Federal Council for Science & Technology
The White House
Washington, D. C. (1)

Dr. H. G. Hopkins
War Office
Armament Research and Development Establishment
Fort Halstead
Sevenoaks, Kent, England (1)

Professor J. E. Cermak
Department of Civil Engineering
Colorado State University
Fort Collins, Colorado (1)

Professor W. J. Hall
Department of Civil Engineering
University of Illinois
Urbana, Illinois (1)

Professor R. Muki
Division of Mechanical Engineering
Keio University
Koganei-shi
Tokyo, Japan (1)